

# Kaon CP violation and neutron EDM in the minimal left-right symmetric model

Stefano Bertolini,<sup>1,\*</sup> Alessio Maiezza,<sup>2,†</sup> and Fabrizio Nesti<sup>3,‡</sup>

<sup>1</sup>*INFN, Sezione di Trieste, SISSA, Via Bonomea 265, 34136 Trieste, Italy*

<sup>2</sup>*Rudjer Boskovic Institute, Division of Theoretical Physics, Bijenička cesta 54, 10000, Zagreb, Croatia*

<sup>3</sup>*Dipartimento di Scienze Fisiche e Chimiche, Università dell’Aquila, via Vetoio SNC, I-67100, L’Aquila, Italy*

Within the minimal Left-Right (LR) symmetric model we revisit the predictions for the kaon CP violating observables  $\varepsilon$  and  $\varepsilon'$  in correlation with those for the neutron electric dipole moment. We perform a complete study of the cross constraints on the model parameters, phases and the  $M_{W_R}$  scale, considering the two cases of parity or charge conjugation as LR discrete symmetries, together with the possible presence of a Peccei-Quinn symmetry. We discuss in particular two scenarios: whether the Standard Model saturates the experimental value of  $\varepsilon'/\varepsilon$  or whether new physics is needed, still an open issue when considering the recent lattice results on the penguin matrix elements. Within the first scenario, we find no constraints on the LR scale in the charge-conjugation case while in the parity case we show that  $M_{W_R}$  can be as low as 14 TeV. On the other hand, the request that new physics contributes dominantly to  $\varepsilon'$  implies strong correlations among the model parameters, with an upper bound of  $M_{W_R} < 10\text{--}100$  TeV in the case of charge conjugation and a range of  $M_{W_R} \simeq 7\text{--}30$  TeV in the parity setup. Both scenarios may be probed directly at future colliders and only indirectly at the LHC.

## I. INTRODUCTION

Flavor phenomenology offers a window for physics beyond the Standard Model (SM). In particular, flavor changing neutral current (FCNC) processes play a key role in the search for new phenomena since they are forbidden at the tree level. For processes involving light quark families, on top of the loop suppression a further reduction results from the smallness of the family quark mass splittings, known as the GIM mechanism [1]. Moreover, CP violation requires the presence of the three families in the loop and therefore of the hierarchically small mixings [2]. The rarity of these processes is indeed a smashing success of the SM setup. Kaon CP-violating (CPV) observables as  $\varepsilon$  and  $\varepsilon'$  belong to this class and are a most sensitive probe for most extensions of the standard electroweak scenario.

A flavor conserving observable that shares a similar discovery potential is the electric dipole moment of the neutron ( $n$ EDM) [3]. It violates parity and time-reversal and therefore CP. In the SM direct electroweak contributions are generated at higher loop order and are well below the present experimental bound ( $2.9 \times 10^{-26}$  e cm [4]). A direct contribution related to the QCD theta-term  $\bar{\theta}$  also induces an  $n$ EDM, which then requires  $\bar{\theta} < 10^{-10}$ .

Such a tiny bound is technically natural in the SM because  $\bar{\theta}$  is perturbatively protected [5], thus avoiding the need for a first principle understanding of its smallness, the so-called strong CP problem. On the other hand, the issue is real in most SM extensions which exhibit new flavor structures and additional CPV phases that lead to potentially large contributions to these observables.

In the present work, we update on the scrutiny of Left-

Right (LR) symmetric theories, based on the gauge group  $\mathcal{G} = SU(2)_L \otimes SU(2)_R \otimes U(1)_{B-L}$  [6–8]. A particular role is played by the minimal version of the Left-Right symmetric models (LRSM) [9]. Besides being predictive, the model provides a natural rationale for the origin and smallness of the neutrino mass [10, 11], a setup for the restoration of parity at high scale [12], and a novel source for neutrinoless double-beta decay [13, 14]. The LRSM has aroused a renewed interest in the era of LHC, because of the possibility of a direct detection via the Keung-Senjanovic (KS) process [15], which violates lepton number in full analogy with the low energy neutrinoless double-beta decay.

The minimality of the model ensures a connection between Majorana and Dirac masses, making it a predictive theory even for neutrinos [16–19]. Since early times the LR scale  $M_{W_R}$  as well as the model parameters were found to be strictly constrained by flavor physics [20, 21]. More recently the possibility of a low LR scale within the LHC reach was emphasized combining bounds from many observables [22]. Subsequent analyses focusing on  $\varepsilon'$  were performed [23, 24] and a lower bound on the LR scale slightly above 3 TeV was finally evinced [25], including the relevant constraints from  $B_{d,s}$  meson oscillations.

The impact of the  $n$ EDM bound on the LRSM requires a separate comment. Exact and spontaneously broken  $\mathcal{P}$  has been considered as a solution of the strong CP problem [26] as an alternative to the dynamical Peccei-Quinn (PQ) mechanism [27–29]. In the case of spontaneously broken  $\mathcal{P}$ ,  $\bar{\theta}$  becomes computable in terms of a single CP-violating parameter. The original argument was revisited in [30] uncovering a large bound on the LR scale of about  $M_{W_R} > 30$  TeV, which pushes the scale beyond the current experimental reach. This conclusion is however specific of the given setup and could be spoiled by envisaging, for instance, the presence of a PQ mechanism so that the LR scale might still be at the reach of LHC.

\* [stefano.bertolini@sissa.it](mailto:stefano.bertolini@sissa.it)

† [Alessio.Maiezza@irb.hr](mailto:Alessio.Maiezza@irb.hr)

‡ [fabrizio.nesti@quila.infn.it](mailto:fabrizio.nesti@quila.infn.it)

Although a scale of  $M_{W_R}$  below 6 TeV is disfavored by the demand that the Higgs sector remains in a perturbative regime [31, 32], an energy window remains for discovery via the KS process [33].

As we shall see, the phase and flavor structure of the LRSM tightly correlates nEDM,  $\varepsilon$  and  $\varepsilon'$ , calling for a detailed study. We shall not enter here the debate on the SM calculations of  $\varepsilon'$  that presently suffer from large uncertainties and leave open the possibility of large new physics contributions [34, 35]. Our analysis will address the different scenarios according to the relevance of the LRSM contributions, addressing the present and future implications.

Previous analyses of these observables with RH currents are available. The works [36, 37] address the problem via an effective theory of RH currents in a model independent way which necessarily misses the detailed phase correlations. Ref. [38] analyzes a specific choice of LR discrete symmetry (the left-right charge conjugation  $\mathcal{C}$ , see below) and we shall compare their findings with our results. In [39], the left-right parity  $\mathcal{P}$  was considered in the limit of decoupled  $W_R$ , where only the flavor-changing heavy scalar contributes, making it effectively a particular two Higgs doublet model. In all cases, the detailed analysis of the correlations among the different observables shows to be relevant.

In summary, we review and reassess the impact of the  $\varepsilon$ ,  $\varepsilon'$  and  $n$ EDM observables on the LRSM, paying attention to the theoretical uncertainties, presently dominated by the hadronic matrix elements, and to the phase patterns and correlations ensuing from either choice of LR symmetry (generalized  $\mathcal{P}$  or  $\mathcal{C}$ ). As far as  $\varepsilon'/\varepsilon$  is concerned, we consider two benchmark cases: i) a scenario in which the SM prediction of  $\varepsilon'$  saturates the experimental result, and ii) a new-physics one where the LRSM contribution is the main source for it.

We conclude that, in the case of  $\mathcal{P}$  the standard scenario imposes a lower bound on the LR scale of  $\sim 14$  TeV, while in the other case a new-physics contribution to  $\varepsilon'$  can arise for  $M_{W_R} = 8\text{--}30$  TeV, with the  $n$ EDM to be at the reach of the new generations of experiments. In the case of  $\mathcal{C}$ , no lower bound arises in the standard scenario, since the relevant phases can be set as small as needed. On the other hand, LR contributions can saturate  $\varepsilon'$  for  $M_{W_R}$  as large as 100 TeV with a given configuration of the model parameters.

The study is organized as follows. In the next section we briefly recall the LRSM features which are relevant for the analysis. In Section III, IV and V we review and update the LRSM contributions to the  $K^0 - \bar{K}^0$  oscillations,  $\varepsilon'/\varepsilon$  and  $n$ EDM respectively, and discuss the status of hadronic matrix elements calculations. In section VI we finally show the outcome of our numerical study. We report in the appendices the relevant tools, namely loop functions, operator anomalous dimensions, meson and baryon chiral Lagrangian, and explicit formulæ for the CP-violating phases in the LRSM.

## II. THE MODEL

### A. The gauge and scalar sectors

The LRSM, with gauge group  $SU(2)_L \times SU(2)_R \times U(1)_{B-L} \times SU(3)_c$ , contains three additional gauge bosons related to the  $SU(2)_R$  group,  $W_R^\pm$  and a new neutral vector  $Z'$ . Left-handed and Right-handed quarks and leptons are accommodated in the fundamental representations of  $SU(2)_{L,R}$ ,  $Q_{L,R} = (u\ d)_{L,R}^t$ ,  $\ell_{L,R} = (\nu\ e)_{L,R}^t$ , with electric charge  $Q = I_{3L} + I_{3R} + \frac{B-L}{2}$ , where  $I_{3L,R}$  are the third generators of  $SU(2)_{L,R}$ . In analogy with the SM, the RH charged currents induce flavor-violating (FV) interactions, and furthermore  $W_R$  mixes with  $W_L$ . This provides a RH interaction mediated by the light mass-eigenstate, mostly the standard gauge boson  $W$ , namely

$$\mathcal{L}_{\text{mix-current}} = \frac{g}{\sqrt{2}} \zeta W^\mu \bar{u}_R V_R \gamma_\mu d_R + h.c. , \quad (1)$$

where  $\zeta$  is the gauge boson mixing to be defined shortly,  $V_R$  is the right-handed equivalent of the standard CKM matrix, and  $u, d$  span the three quark flavors.

The  $SU(2)_R \times U(1)_{B-L} \rightarrow U(1)_Y$  spontaneous symmetry breaking is provided by a RH triplet  $\Delta_R(1_L, 3_R, 2)$

$$\Delta_R = \begin{bmatrix} \Delta^+/\sqrt{2} & \Delta^{++} \\ \Delta^0 & -\Delta^+/\sqrt{2} \end{bmatrix}_R , \quad (2)$$

via the vacuum expectation value (VEV)  $v_R$  developed by  $\Delta^0$ . Then the  $W_R$  gauge boson has mass  $M_{W_R} = gv_R$ .

The LR mixing  $\zeta$  between  $W_R$  and  $W \simeq W_L$  is

$$\zeta \simeq -r e^{i\alpha} \sin 2\beta , \quad (3)$$

with  $r = M_{W_L}^2/M_{W_R}^2$  and  $\tan \beta \equiv t_\beta = v_2/v_1$ . From the direct experimental limit on the LR scale one obtains  $|\zeta| < 4 \times 10^{-4}$ . Here  $v_{1,2}$  are related to the electroweak breaking, provided by a bidoublet field  $\Phi(2_L, 2_R, 0)$

$$\Phi = \begin{bmatrix} \phi_1^0 & \phi_2^+ \\ \phi_1^- & \phi_2^0 \end{bmatrix} . \quad (4)$$

with VEV  $\langle \Phi \rangle = \text{diag} \{v_1, e^{i\alpha} v_2\}$  [12]. The standard electroweak VEV is given by  $v^2 = v_1^2 + v_2^2$ , with  $v \ll v_R$ . The standard Higgs boson is contained in (4) predominantly in the real part of  $\phi_1$ ; the imaginary and complex components of  $\phi_2$  are instead neutral scalars whose masses are proportional to  $v_R$ . They have to be heavy enough because they mediate tree-level FCNC, and their presence plays an important role in the phenomenology of the low-scale LRSM.

For the present study devoted to the CP observables  $\varepsilon$ ,  $\varepsilon'/\varepsilon$  and  $n$ EDM, one of the main ingredients is Eq. (1). It contains sources of CP-violation because of the spontaneous phase  $\alpha$  inside  $\zeta$  and of the complexity of  $V_R$ . Remarkably, a tree-level contribution to  $\varepsilon'$  is generated by the LR mixing  $\zeta$  via an effective four-quark operator

(defined below as  $Q_2^{LR}$ ) obtained after integration of the gauge field. The complete basis of operators, induced at tree or loop level and through renormalization to low scale, will be listed in section IV. A similar treatment is reserved for  $n$ EDM, in the case of  $\Delta S = 0$  transitions: as we shall see, analogous effective operators generate via chiral loops the dominant contribution to the  $n$ EDM [30]. The account and evaluation of the various sources of  $\varepsilon'$  and  $n$ EDM are the matter of dedicated sections in the following.

## B. The choice of LR discrete symmetry

In Eq. (1) the condition  $g_L = g_R = g$  is assumed, being  $g_{L,R}$  the gauge coupling of  $SU(2)_{L,R}$ . This follows from an additional discrete symmetry in the LRSR relating the left and right sector. Such a symmetry is not unique: it can be realized either with a generalized parity  $\mathcal{P}$  or a generalized charge conjugation  $\mathcal{C}$  which, in addition to exchanging the weak gauge groups, are defined respectively by [22]

$$\mathcal{P} : \begin{cases} Q_L \leftrightarrow Q_R \\ \Phi \rightarrow \Phi^\dagger \end{cases}, \quad \mathcal{C} : \begin{cases} Q_L \leftrightarrow (Q_R)^c \\ \Phi \rightarrow \Phi^T \end{cases}, \quad (5)$$

with analogous transformationa for the lepton doublets. The action of  $\mathcal{P}$  and  $\mathcal{C}$  on the Yukawa Lagrangian

$$\mathcal{L}_Y = \bar{Q}_L (Y \Phi + \tilde{Y} \tilde{\Phi}) Q_R + h.c., \quad (6)$$

implies  $Y = Y^\dagger$  and  $Y = Y^T$  respectively, and the same for  $\tilde{Y}$ . After the quark mass matrices

$$\begin{aligned} M_u &= v_1 Y + v_2 e^{-i\alpha} \tilde{Y} \\ M_d &= v_2 e^{i\alpha} Y + v_1 \tilde{Y} \end{aligned} \quad (7)$$

are bi-diagonalized given forms of  $V_R$  are obtained, according to the properties of  $Y, \tilde{Y}$ . The case of  $\mathcal{C}$  is fairly simple [22]:

$$V_R = K_u V^* K_d, \quad (8)$$

with  $V$  the standard CKM matrix and  $K_{u,d}$  diagonal matrices of free phases  $K_u = \text{diag}\{e^{i\theta_u}, e^{i\theta_c}, e^{i\theta_t}\}$ ,  $K_d = \text{diag}\{e^{i\theta_d}, e^{i\theta_s}, e^{i\theta_b}\}$ , where from now on we adopt  $\theta_b = 0$ .

In the case of  $\mathcal{P}$ , an analytical form for  $V_R$  has been recently found, with a perturbative expansion in the small parameter  $|s_\alpha t_{2\beta}| \lesssim 2m_b/m_t \simeq 0.05$  [40, 41]:

$$\begin{aligned} V_R = & V_{ij} - i s_\alpha t_{2\beta} \left( V_{ij} t_\beta + \sum_{k=1}^3 \frac{V_{kj} (V m_d V^\dagger)_{ik}}{m_{u\,ii} + m_{u\,kk}} \right. \\ & \left. + \frac{V_{ik} (V^\dagger m_u V)_{kj}}{m_{d\,jj} + m_{d\,kk}} \right) + \mathcal{O}(s_\alpha t_{2\beta})^2, \end{aligned} \quad (9)$$

where  $m_{u,d}$  are the diagonal quark mass matrices. This expression is not unique, other solutions are found by replacing  $m_{ii} \rightarrow s_i m_{ii}$  and

$$V \rightarrow \text{diag}\{s_u, s_c, s_t\} V \text{diag}\{s_d, s_s, s_b\}, \quad (10)$$

where  $s_i$  are arbitrary signs (and from now on we adopt  $s_b = 1$ ). In Appendix A, explicit expressions for the relevant phase combinations are given for generic  $s_i$ .

The argument of the determinant of the fermion mass matrices can also be computed [30, 40, 41], namely

$$\bar{\theta} \simeq \frac{1}{2} s_\alpha t_{2\beta} \text{tr} (m_u^{-1} V m_d V^\dagger - m_d^{-1} V^\dagger m_u V), \quad (11)$$

at the first order in  $s_\alpha t_{2\beta}$ .

## III. $K^0 - \bar{K}^0$ MIXING

A particularly constraining process for the LRSR is the neutral kaon mixing, effectively induced through the chirally enhanced operator

$$\langle \bar{K}^0 | \bar{s} L d \bar{s} R d | K^0 \rangle = \frac{1}{2} f_K^2 m_K \mathcal{B}_4^K \left[ \frac{m_K^2}{(m_s + m_d)^2} + \frac{1}{6} \right], \quad (12)$$

where  $f_K$  and  $m_K$  are the decay constant and the mass of the meson  $K$  respectively, and  $L, R = (1 \mp \gamma_5)/2$ . This operator is generated via the LR box diagrams and even at the tree-level through the exchange of a flavor-changing (FC) scalar [12, 42]. The inclusion of the one-loop renormalization of the tree-level diagrams, necessary for a gauge invariant result [43], has phenomenologically relevant implications [25]. The bag factor  $\mathcal{B}_4^K$  has been computed on the lattice by various groups with some 20% discrepancies [44]. For the present study, we follow the discussion and numerical analysis of Ref. [25], to which we refer the reader for the details.

The CP violating parameter  $\varepsilon$ , which gauges the indirect CP violation in the mixing, is particularly important in constraining the external CP-phases introduced in the previous section [22, 25]. The bounds may be inferred by using a convenient parametrization of new physics in  $\varepsilon$ , namely

$$h_\varepsilon \equiv \frac{\text{Im} \langle \bar{K}^0 | \mathcal{H}_{LR} | K^0 \rangle}{\text{Im} \langle \bar{K}^0 | \mathcal{H}_{LL} | K^0 \rangle}, \quad (13)$$

which in the case of  $\mathcal{C}$  turns into

$$h_\varepsilon^{\mathcal{C}} \simeq \text{Im} \left[ e^{i(\theta_d - \theta_s)} (A_{cc} + A_{ct} \cos(\theta_c - \theta_t + \phi)) \right], \quad (14)$$

while in the case of  $\mathcal{P}$  becomes

$$h_\varepsilon^{\mathcal{P}} \propto \text{Im} \left[ e^{i(\theta_d - \theta_s)} [A_{cc} + A_{ct} e^{i\phi} \cos(\theta_c - \theta_t)] \right], \quad (15)$$

with  $\phi = \arg(V_{Ltd}) \simeq -22^\circ$ .  $A_{cc,ct}$  correspond to the contributions of charm-charm and charm-top quark in the effective Lagrangian. They are real numbers which scale circa as  $M_{W_R}^{-2}$ , as we consider the contribution of the FC scalar to be at most comparable to the one of  $M_{W_R}$ , corresponding to  $M_H \simeq 6M_{W_R}$  within the perturbative regime [25]. For a wide range of  $M_{W_R}$  one has  $A_{ct}/A_{cc} \simeq 0.45$ .

Conservatively we allow the amount of new physics in  $\varepsilon$  to be at most 10% [45]. This translates into a sharp constraint on  $\theta_d - \theta_s$  [25], which in the case of  $\mathcal{C}$  reads

$$\begin{aligned} |\sin(\theta_s - \theta_d)|_{s_c s_t = -1} &< \left( \frac{M_{W_R}}{104 \text{ TeV}} \right)^2 \\ |\sin(\theta_s - \theta_d)|_{s_c s_t = 1} &< \left( \frac{M_{W_R}}{71 \text{ TeV}} \right)^2, \end{aligned} \quad (16)$$

while for  $\mathcal{P}$  one has

$$\begin{aligned} |\sin(\theta_s - \theta_d + 0.16)|_{s_c s_t = -1} &< \left( \frac{M_{W_R}}{104 \text{ TeV}} \right)^2 \\ |\sin(\theta_s - \theta_d - 0.16)|_{s_c s_t = 1} &< \left( \frac{M_{W_R}}{71 \text{ TeV}} \right)^2. \end{aligned} \quad (17)$$

## IV. DIRECT CP VIOLATION IN $K^0 \rightarrow \pi\pi$

### A. Effective interactions

Mesonic and hadronic processes that involve weak interactions are best described in terms of the operator product expansion, which factorizes short- and long-distance effects. For  $\Delta S = 1$  flavor changing transitions the effective Lagrangian can be written in the form

$$L_{\Delta S=1} = -\frac{G_F}{\sqrt{2}} \sum_i C_i Q_i + h.c., \quad (18)$$

where  $Q_i$  are the relevant operators and  $C_i$  the corresponding Wilson coefficients ( $G_F$  is the Fermi constant).

In the Standard Model the  $\Delta S = 1$  Lagrangian involves tree-level operators as well as QED and QCD induced loop diagrams. When both left and right chirality interactions are present, the standard set of operators is enlarged to include, at the scale of 1 GeV, 28 operators [23]

$$\begin{aligned} Q_1^{LL} &= (\bar{s}_\alpha u_\beta)_L (\bar{u}_\beta d_\alpha)_L & Q_1^{RR} &= (\bar{s}_\alpha u_\beta)_R (\bar{u}_\beta d_\alpha)_R \\ Q_2^{LL} &= (\bar{s}_\alpha)_L (\bar{u} d)_L & Q_2^{RR} &= (\bar{s}_\alpha)_R (\bar{u} d)_R \\ Q_3 &= (\bar{s} d)_L (\bar{q} q)_L & Q'_3 &= (\bar{s} d)_R (\bar{q} q)_R \\ Q_4 &= (\bar{s}_\alpha d_\beta)_L (\bar{q}_\beta q_\alpha)_L & Q'_4 &= (\bar{s}_\alpha d_\beta)_R (\bar{q}_\beta q_\alpha)_R \\ Q_9 &= \frac{3}{2} (\bar{s} d)_L e_q (\bar{q} q)_L & Q'_9 &= \frac{3}{2} (\bar{s} d)_R e_q (\bar{q} q)_R \\ Q_{10} &= \frac{3}{2} (\bar{s}_\alpha d_\beta)_L e_q (\bar{q}_\beta q_\alpha)_L & Q'_{10} &= \frac{3}{2} (\bar{s}_\alpha d_\beta)_R e_q (\bar{q}_\beta q_\alpha)_R \end{aligned} \quad (19)$$

$$\begin{aligned} Q_1^{RL} &= (\bar{s}_\alpha u_\beta)_R (\bar{u}_\beta d_\alpha)_L & Q_1^{LR} &= (\bar{s}_\alpha u_\beta)_L (\bar{u}_\beta d_\alpha)_R \\ Q_2^{RL} &= (\bar{s}_\alpha)_R (\bar{u} d)_L & Q_2^{LR} &= (\bar{s}_\alpha)_L (\bar{u} d)_R \\ Q_5 &= (\bar{s} d)_L (\bar{q} q)_R & Q'_5 &= (\bar{s} d)_R (\bar{q} q)_L \\ Q_6 &= (\bar{s}_\alpha d_\beta)_L (\bar{q}_\beta q_\alpha)_R & Q'_6 &= (\bar{s}_\alpha d_\beta)_R (\bar{q}_\beta q_\alpha)_L \\ Q_7 &= \frac{3}{2} (\bar{s} d)_L e_q (\bar{q} q)_R & Q'_7 &= \frac{3}{2} (\bar{s} d)_R e_q (\bar{q} q)_L \\ Q_8 &= \frac{3}{2} (\bar{s}_\alpha d_\beta)_L e_q (\bar{q}_\beta q_\alpha)_R & Q'_8 &= \frac{3}{2} (\bar{s}_\alpha d_\beta)_R e_q (\bar{q}_\beta q_\alpha)_L \end{aligned} \quad (20)$$

$$\begin{aligned} Q_g^L &= \frac{g_s m_s}{16\pi^2} \bar{s} \sigma_{\mu\nu} t^a G_a^{\mu\nu} L d & Q_g^R &= \frac{g_s m_s}{8\pi^2} \bar{s} \sigma_{\mu\nu} t^a G_a^{\mu\nu} R d \\ Q_\gamma^L &= \frac{e m_s}{16\pi^2} \bar{s} \sigma_{\mu\nu} F_a^{\mu\nu} L d & Q_\gamma^R &= \frac{e m_s}{8\pi^2} \bar{s} \sigma_{\mu\nu} F_a^{\mu\nu} R d, \end{aligned} \quad (21)$$

with  $(\bar{q} q)_{L,R} \equiv \bar{q} \gamma_\mu (L,R) q$ ,  $L, R \equiv 1 \mp \gamma_5$ , and implicit summation on  $q = u, d, s$ .  $Q_{1,2}^{LL}$  are the SM operators usually denoted as  $Q_{1,2}$ . The dipole operators  $Q_{g,\gamma}$  are normalized with  $m_s$ , for an easy comparison with existing calculations and anomalous dimensions. It is known that some of the operators above are characterized by enhancements due to their chiral structure, either in the running of the short distance coefficient or in the matrix element. In particular the Wilson coefficients of the QCD dipole operators  $Q_g^{L,R}$  receive a large enhancement from the mixing with the current-current operators.

At the leading order the operators generated by the SM and the LR short distance physics are:  $Q_2^{AB}$ ,  $Q_4$ ,  $Q'_4$ ,  $Q_6$ ,  $Q'_6$ ,  $Q_7$ ,  $Q'_7$ ,  $Q_9$ ,  $Q'_9$ ,  $Q_g^A$ ,  $Q_\gamma^A$ , with  $A, B = L, R$ . Their Wilson coefficients are for current-current operators

$$\begin{aligned} C_2^{LL} &= \lambda_u^{LL}, & C_2^{LR} &= \zeta^* \lambda_u^{LR}, \\ C_2^{RR} &= r \lambda_u^{RR}, & C_2^{RL} &= \zeta \lambda_u^{RL}; \end{aligned} \quad (22)$$

for the penguins

$$\begin{aligned} C_4 &= C_6 = \frac{\alpha_s}{4\pi} \sum_i \lambda_i^{LL} F_1^{LL}(x_i) \\ C'_4 &= C'_6 = \frac{\alpha_s}{4\pi} r \sum_i \lambda_i^{RR} F_1^{RR}(rx_i) \\ C_7 &= C_9 = \frac{\alpha e_u}{4\pi} \sum_i \lambda_i^{LL} E_1^{LL}(x_i) \\ C'_7 &= C'_9 = \frac{\alpha e_u}{4\pi} r \sum_i \lambda_i^{RR} E_1^{RR}(rx_i); \end{aligned} \quad (23)$$

and for the dipoles

$$\begin{aligned} m_s C_g^L &= \sum_i \left[ m_s \lambda_i^{LL} F_2^{LL} + \zeta m_i \lambda_i^{RL} F_2^{LR} + m_d r \lambda_i^{RR} F_2^{RR} \right] \\ m_s C_g^R &= \sum_i \left[ m_d \lambda_i^{LL} F_2^{LL} + \zeta^* m_i \lambda_i^{LR} F_2^{LR} + m_s r \lambda_i^{RR} F_2^{RR} \right] \\ m_s C_\gamma^L &= \sum_i \left[ m_s \lambda_i^{LL} E_2^{LL} + \zeta m_i \lambda_i^{RL} E_2^{LR} + m_d r \lambda_i^{RR} E_2^{RR} \right] \\ m_s C_\gamma^R &= \sum_i \left[ m_d \lambda_i^{LL} E_2^{LL} + \zeta^* m_i \lambda_i^{LR} E_2^{LR} + m_s r \lambda_i^{RR} E_2^{RR} \right]. \end{aligned} \quad (24)$$

In the above,  $e_u = 2/3$  is the  $u$ -quark charge,  $x_i = m_i^2/m_{W_L}^2$  with  $i = u, c, t$ , and  $F_{1,2}^{AB}$  and  $E_{1,2}^{AB}$  are the loop functions, given in appendix B. The parameters  $\zeta$  and  $r$  are defined in Eq. (3). Finally  $\lambda_i^{AB} = V_{is}^{*A} V_{id}^B$ , where  $V_L$  and  $V_R$  are the Cabibbo-Kobayashi-Maskawa (CKM) matrix and its right-handed analogue (Eqs. (8)–(9)).

The different terms of the coefficients in Eqs. (22)–(24) are generated at the decoupling of the relevant heavy thresholds, and thus at different scales, namely  $M_{W_L}$  or  $m_t$  for the current-current operators and top-dominated loops,  $m_c$  for the charm dominated loops, and  $m_{W_R}$  for the RR current-current ones.

The direct CP violation in  $K^0 \rightarrow \pi\pi$  decays is parametrised as

$$\text{Re} \frac{\varepsilon'}{\varepsilon} \simeq \frac{\omega}{\sqrt{2} |\varepsilon|} \left( \frac{\text{Im} A_2}{\text{Re} A_2} - \frac{\text{Im} A_0}{\text{Re} A_0} \right), \quad (25)$$

where  $\omega = \text{Re} A_2 / \text{Re} A_0 \simeq 1/22.2$ . The isospin amplitudes  $A_I$  ( $I = 0, 2$ ) are defined from the  $\Delta S = 1$  effective Hamiltonian as  $\langle (2\pi)_I | (-i)H_{\Delta S=1} | K^0 \rangle = A_I e^{i\delta_I}$ , where  $\delta_I$  are the strong phases of  $\pi\pi$  scattering. The phase of  $\varepsilon', \pi/2 + \delta_2 - \delta_0 = 42.5^\circ \pm 0.9^\circ$ , cancels to a very good approximation the phase of  $\varepsilon$ .

While the imaginary part of the amplitudes are calculated within the model, the real parts are set at their experimental values:  $\text{Re} A_0 = 3.33 \times 10^{-7}$  GeV and  $\text{Re} A_2 = 1.49 \times 10^{-8}$  GeV, as well as the indirect CP violation parameter  $|\varepsilon| = (2.228 \pm 0.011) \times 10^{-3}$ . Because of the large uncertainty associated to the new physics contribution to  $\varepsilon'$  we neglect in Eq. (25) a  $O(10\%)$  isospin breaking correction (for a recent recap on isospin violation in the SM amplitudes see Ref. [34]). As a matter of fact, the major source of uncertainty resides in the evaluation of the hadronic matrix elements, that we are going to discuss next.

For the following discussion and numerical analysis it is convenient to introduce the parameter

$$h_{\varepsilon'} = \frac{\varepsilon'_{LR}}{\varepsilon'_{\text{exp}}}, \quad (26)$$

where  $\varepsilon'_{LR}$  represents the additional LRSM contribution to  $\varepsilon'$ , and is normalized to the present experimental central value,  $|\varepsilon'_{\text{exp}}| = 3.7 \times 10^{-6}$ .

## B. Matrix elements

In this section we address the evaluation of the  $K^0 \rightarrow \pi\pi$  matrix elements of the left-right current-current operators  $Q_{1,2}^{LR}$ . We define  $\langle Q_i^{LR} \rangle_{0,2} \equiv \langle (\pi\pi)_{I=0,2} | Q_i^{LR} | K^0 \rangle$ . A naive estimate is provided by the simple factorization of the matrix elements in terms of currents and densities and vacuum insertion known as the Vacuum Saturation Approximation (VSA) [46]. In spite of the expected large non factorizable corrections the VSA has been conveniently used in the past as a reference benchmark. The calculation of the current-current operators in the left-right framework via the VSA prescription is found in [21]. In terms of the  $Q_{1,2}^{LR}$  operators defined above one has

$$\begin{aligned} \langle Q_1^{LR} \rangle_0 &= -\langle Q_1^{RL} \rangle_0 = -\frac{1}{3} \sqrt{\frac{2}{3}} (X + 9Y + 3Z) \\ \langle Q_1^{LR} \rangle_2 &= -\langle Q_1^{RL} \rangle_2 = -\frac{1}{3} \sqrt{\frac{1}{3}} (X - 6Z) \\ \langle Q_2^{LR} \rangle_0 &= -\langle Q_2^{RL} \rangle_0 = -\frac{1}{3} \sqrt{\frac{2}{3}} (3X + 3Y + Z) \\ \langle Q_2^{LR} \rangle_2 &= -\langle Q_2^{RL} \rangle_2 = -\frac{1}{3} \sqrt{\frac{1}{3}} (3X - 2Z), \end{aligned} \quad (27)$$

|                              | VSA   | $\chi$ QM | DQCD   |
|------------------------------|-------|-----------|--------|
| $\langle Q_1^{LR} \rangle_0$ | -1.8  | -3.6      | -1.1   |
| $\langle Q_1^{LR} \rangle_2$ | 0.53  | 0.33      | 0.40   |
| $\langle Q_2^{LR} \rangle_0$ | -0.62 | -1.2      | -0.059 |
| $\langle Q_2^{LR} \rangle_2$ | 0.16  | 0.092     | -0.005 |

TABLE I. Comparison of  $K^0 \rightarrow \pi\pi$  matrix elements of the left-right current-current operators  $Q_{1,2}^{LR}$  in different approaches. The values are given at the scale of 1 GeV in units of  $\text{GeV}^3$  for central values of the relevant input parameters.

with

$$\begin{aligned} X &\equiv i \langle \pi^+ | \bar{u} \gamma_\mu \gamma_5 d | 0 \rangle \langle \pi^- | \bar{s} \gamma^\mu u | K^0 \rangle \simeq \sqrt{2} f_\pi (m_K^2 - m_\pi^2) \\ Y &\equiv i \langle \pi^+ \pi^- | \bar{u} u | 0 \rangle \langle 0 | \bar{s} \gamma_5 d | K^0 \rangle \simeq \sqrt{2} f_K m_K^4 / (m_s + m_d)^2 \\ Z &\equiv i \langle \pi^+ | \bar{u} \gamma_5 d | 0 \rangle \langle \pi^- | \bar{s} u | K^0 \rangle \simeq \sqrt{2} f_\pi m_K^4 / (m_s + m_d)^2. \end{aligned} \quad (28)$$

At variance with [21] in Eq. (28) a factor  $i$  is conventionally factored out. When allowed, charged pions are replaced by neutral pions with a factor of 2 accounting for their exchange, so that for instance  $iZ = 2 \langle \pi^0 | \bar{u} \gamma_5 u | 0 \rangle \langle \pi^0 | \bar{s} d | K^0 \rangle$ . The term  $Y$  contributes equally to charged and neutral pions and accordingly it is absent in the isospin 2 projection of the amplitudes

$$\begin{aligned} A_0 &= \frac{1}{\sqrt{6}} (2A_\pm + A_{00}), \\ A_2 &= \frac{1}{\sqrt{3}} (A_\pm - A_{00}). \end{aligned} \quad (29)$$

In Eq. (27) non leading terms in  $1/N$  due to color Fierz are kept according to the VSA prescription. For  $Q_2^{LR}$  the  $1/N$  terms  $Y$  and  $Z$  are chirally enhanced and dominate the amplitude, that turns out to be approximately  $1/3$  of the corresponding one of  $Q_1^{LR}$ . The VSA values in Table I are given at the scale of 1 GeV with  $(m_s + m_d)(1 \text{ GeV}) \approx 132 \text{ MeV}$ .

In the second column we report the results of the computation of the  $K^0 \rightarrow \pi\pi$  matrix elements of  $Q_{1,2}^{LR}$  within the Chiral Quark Model ( $\chi$ QM) approach [23, 24]. In this modeling of low energy QCD the meson octet chiral Lagrangian is complemented with an effective quark-meson interaction [47, 48], which provides a connection between the QCD degrees of freedom and the lightest hadronic states. Meson interactions are then obtained by integration of the constituent quarks and the chiral Lagrangian coefficients are determined in terms of three non-perturbative parameters, namely the constituent quark mass, and the quark and gluon condensates.

In the nineties an extensive program was carried out in order to calculate all  $\Delta S = 1$  matrix elements relevant to the  $\Delta I = 1/2$  rule and direct CP violation in  $K^0 \rightarrow \pi\pi$  decays based on the  $\chi$ QM at the NLO in the chiral expansion [49]. By adopting a phenomenological approach

it was shown that a fit of the  $\Delta I = 1/2$  rule could be obtained for expected values of the three non-perturbative parameters of the model.<sup>1</sup> [50] In turn, this allowed a coherent calculation of the matrix elements for the whole dimension six  $\Delta S = 1$  SM Lagrangian[51], including the dimension five chromomagnetic dipole operator [52, 53].<sup>2</sup>

The relevance of non-factorizable  $1/N$  model and chiral corrections in lifting the cancellation between the gluon and electromagnetic penguin was exposed, leading in 1998 to the prediction  $\varepsilon'/\varepsilon = 17^{+17}_{-10} \times 10^{-4}$  [56, 57] shortly afterwards confirmed by the precise experimental findings of KTEV [58] and NA48 [59] collaborations

$$\varepsilon'/\varepsilon = 16.6 \pm 2.3 \times 10^{-4} \quad (30)$$

Subsequent attempts to resum the final state interactions via dispersion relations [60–64] lead to a confirmation of the enhancement of the  $I = 0$  amplitudes and of the agreement between SM and data.

In recent years the phenomenological  $\chi$ QM framework has been applied to the calculation of the matrix elements of relevant operators in the left-right model [24]. In Table I the matrix elements of  $Q_{1,2}^{LR}$  obtained in the model at the scale of 0.8 GeV are evolved to 1 GeV. As remarked in [24], attention must be paid in subtracting an unphysical contribution to the  $K^0 \rightarrow \pi\pi$  amplitudes generated by the presence of a  $K^0 \rightarrow$  vacuum transition (tadpole) [65] induced by the LR current-current operators. We see again in the  $\chi$ QM calculation an enhancement of the  $\Delta I = 1/2$  amplitudes compared to the  $\Delta I = 3/2$  ones. This pattern is lead by the one-loop chiral loop contributions, which include the final state rescattering.<sup>3</sup>

In the third column of Table I we report the results obtained with the Dual QCD (DQCD) approach [67] (for a recent summary and references see Ref. [35]). A rescaling factor of  $\sqrt{3/2}$  has been applied in order to normalize the DQCD results to the amplitudes defined in Eq. (29). The DQCD calculation of the hadronic matrix elements is based on a truncated chiral Lagrangian and leading  $N$  factorization [68–70]. The matrix elements of the four quark operators are calculated in the large  $N$  limit at zero momentum by factorizing the four quark operators in terms of color singlet currents or densities via their chiral representations. The meson operators undergo an evolution quadratic in the cutoff scale up to  $\Lambda \simeq 0.7$  GeV [71]. They are then matched with the short-distance Wilson coefficients at the 1 GeV scale.

This approach has shown to be successful in the past in predicting the size of the bag parameter  $B_K$  in

$\bar{K}^0 - K^0$  mixing [72, 73] in agreement with lattice calculations. [74, 75] Recently, by supporting (and providing a model rationale for [76]) the RBC-UKQCD lattice results [77, 78] for the  $\Delta I = 1/2$  rule and the direct CP violation in  $K^0 \rightarrow \pi\pi$  decays, leading to

$$\varepsilon'/\varepsilon = 1.38 \pm 6.90 \times 10^{-4}. \quad (31)$$

In spite of the enormous progress made in the past decade, the present lattice calculations of the  $K \rightarrow \pi\pi$  matrix elements still fail in reproducing the strong rescattering phase  $\delta_0$  (by about  $3\sigma$ ) and do not include isospin breaking.<sup>4</sup> It is fair to say that, given the delicate cancellation between the QCD and QED penguin operators that leads to the present SM estimate, we should await for a comprehensive and precise lattice description of the  $K \rightarrow \pi\pi$  decays before claiming the need of new physics explanations.

On the other hand, a detailed reevaluation of  $\varepsilon'/\varepsilon$  within the chiral Lagrangian framework, including isospin breaking, leads to [34]

$$\varepsilon'/\varepsilon = 15 \pm 7 \times 10^{-4} \quad (32)$$

in agreement, albeit with a large error, with the data.<sup>5</sup>

In Table I the values of the relevant matrix elements are reported at the scale of 1 GeV for our operator basis. It is apparent in the comparison the reduced size of  $\langle Q_1^{LR} \rangle_0$  and the minuscule size of the  $Q_2^{LR}$  matrix elements. These results stem from the large  $N$  factorization of the current-current operator (corresponding to the subleading term  $X$  in Eq. (28)). The meson evolution of the  $Q_2^{LR}$  operator mixes it with the chirally enhanced  $Q_1^{LR}$  but with a renormalization suppression factor of  $\Lambda^2/(4\pi f_\pi)^2$ , so that  $1/N$  chirally enhanced terms turn out to be not effective. This is a distinctive feature of the DQCD approach.

The authors of Ref. [38] invoke isospin symmetry to provide a connection between the  $Q_{1,2}^{LR}$  matrix elements and the analogues of the SM gluon and electromagnetic penguins  $Q_{5,6,7,8}$ , for which lattice calculation are available at a scale of 3 GeV. No numerical details are given in [38]. We find that the  $Q^{LR}$  matrix elements so derived follow quite nearly the pattern and size of the VSA results.

Given the spread and pattern of values in Table I we conservatively use in our analysis the results of VSA as a reference benchmark, while including a conservative theoretical uncertainty of a factor of two.

<sup>1</sup> Model dependent non-factorizable  $1/N$  corrections proportional to the gluon condensate were shown to play a crucial role in depleting the isospin 2 amplitude while contributing to the enhancement of the isospin 0 amplitude.

<sup>2</sup> Very recent lattice [54] and QCD model [55] calculations of the gluon dipole operator give a  $K^0 \rightarrow \pi\pi$  matrix element smaller by about a factor of two [23].

<sup>3</sup> The impact of final-state interactions in  $\varepsilon'/\varepsilon$  has been recently questioned in [66]

<sup>4</sup> The role of isospin breaking contributions in the lattice calculations has been further scrutinized in [79].

<sup>5</sup> A very recent update based on a detailed reassessment of the isospin breaking effects leads to  $\varepsilon'/\varepsilon = 14 \pm 5 \times 10^{-4}$  [80].

## V. NEUTRON EDM

### A. Strong CP in LRSM

While the SM provides a natural answer to the smallness of  $\bar{\theta}$ , the latter being perturbatively protected [5], more general approaches have been proposed, which are relevant for new physics extensions. The Peccei-Quinn (PQ) axion models [27–29] provide an elegant way to address dynamically the problem. On the other hand other solutions involving the UV completion are possible, as the restoration of a mirror symmetry in the fermion sector [81].

Within the LRSM such a solution is provided by the scenario in which the  $\mathcal{P}$  symmetry is exact at high scale and only spontaneously broken [26]. The symmetry sets to zero the topological term  $\theta$ , so that  $\bar{\theta}$  is computable after spontaneous breaking, see Eq. (11). Since this is by far the dominant contribution to  $d_n$ , the constraint on  $\bar{\theta}$  translates into a very stringent limit on the combination  $s_\alpha t_{2\beta}$  and thus into the effective vanishing of all phases  $\theta_i$ , which are directly driven by it. In such a situation the  $\varepsilon$  constraint in Eq. (17) implies a lower bound on the LR scale,  $M_{W_R} \gtrsim 28$  TeV [30], as derived from Eq. (17) in the limit  $\theta_s - \theta_d \rightarrow 0$  [25]. This conclusion is avoided if  $\bar{\theta}$  is canceled independently by a mechanism like the PQ one. In the case of LRSM with  $\mathcal{C}$ , both  $\arg \det M$  and  $\theta_{QCD}$  are free parameters, and if one does not want to exploit this freedom as a fine-tuning, the  $\bar{\theta}$  issue has again to be addressed by assuming some underlying mechanism.

After the PQ mechanism removes  $\bar{\theta}$ , still the presence of P- and CP-violating LR effective operators generates various sources of the nEDM [82], in both the  $\mathcal{C}$  and  $\mathcal{P}$  cases. We review and compare their impact in the following sections. It turns out that the most relevant contribution to  $d_n$  is due to meson loops after the shift of the pion field in the chiral Lagrangian, induced by the presence of the CP-violating four-quark operators (see Appendix D). As we will see, within the uncertainties, the final result is fairly insensitive to the detailed mechanism invoked for the cancelation of  $\bar{\theta}$ .

In the following sections we briefly review the contributions to the neutron EDM, arising in the LRSM, from short- and long-distance sources.

### B. Effective operators

The effective CP odd Lagrangian relevant for the nEDM can be written as [83, 84]

$$\mathcal{L}_{EDM} = -\frac{G_F}{\sqrt{2}} \left( \sum_{q \neq q', i=1}^2 \mathcal{C}_i^{qq'} \mathcal{O}_i^{qq'} + \frac{1}{2} \sum_{q \neq q', i=3}^4 \mathcal{C}_i^{qq'} \mathcal{O}_i^{qq'} + \sum_{q, i=1}^4 \mathcal{C}_i^q \mathcal{O}_i^q + \mathcal{C}_5 \mathcal{O}_5 \right), \quad (33)$$

where  $q = u, d$  and the effective operators are given by

$$\mathcal{O}_1^{qq'} = \bar{q} q \bar{q}' i \gamma_5 q', \quad \mathcal{O}_2^{qq'} = \bar{q}_\alpha q_\beta \bar{q}'_\beta i \gamma_5 q'_\alpha, \quad (34)$$

$$\mathcal{O}_3^{qq'} = \bar{q} \sigma^{\mu\nu} q \bar{q}' \sigma_{\mu\nu} i \gamma_5 q', \quad (35)$$

$$\mathcal{O}_4^{qq'} = \bar{q}_\alpha \sigma^{\mu\nu} q_\beta \bar{q}'_\beta \sigma_{\mu\nu} i \gamma_5 q'_\alpha, \quad (36)$$

$$\mathcal{O}_1^q = \bar{q} q \bar{q} i \gamma_5 q, \quad \mathcal{O}_2^q = \bar{q} \sigma_{\mu\nu} q \bar{q} \sigma^{\mu\nu} i \gamma_5 q, \quad (37)$$

$$\mathcal{O}_3^q = -\frac{e}{16\pi^2} e_q m_q \bar{q} \sigma_{\mu\nu} i \gamma_5 q F^{\mu\nu}, \quad (38)$$

$$\mathcal{O}_4^q = -\frac{g_s}{16\pi^2} m_q \bar{q} \sigma_{\mu\nu} i \gamma_5 T^a q G^{a\mu\nu}, \quad (39)$$

$$\mathcal{O}_5 = -\frac{1}{3} \frac{g_s}{16\pi^2} f^{abc} G_{\mu\sigma}^a G_{\nu}^{b,\sigma} \tilde{G}^{c,\mu\nu}, \quad (40)$$

The tensor operators  $\mathcal{O}_{3,4}^{q'q}$  are symmetric in  $q'q$  ( $i\gamma_5 \sigma^{\mu\nu} \propto \varepsilon^{\mu\nu\alpha\beta} \sigma_{\alpha\beta}$ ), hence the factor 1/2 in Eq. (33). The  $\mathcal{O}_{1,2}^{q'q}$  and dipole operators  $\mathcal{O}_{3,4}^q$  are obtained from the  $\Delta S = 1$  Lagrangian Eqs. (18)–(21) by replacing  $s \rightarrow d$ . Accordingly, one finds that the Wilson coefficients  $C_{1,2}^{q'q}$  at the weak scale are related to the  $\Delta S = 1$  ones by

$$C_{1,2}^{ud} = -C_{1,2}^{du} = 4 \text{Im} C_{1,2}^{RL}, \quad (41)$$

while

$$m_{u,d} e_{u,d} C_3^{u,d} = 2m_s \text{Im} (C_\gamma^{R,L}), \quad (42)$$

$$m_{u,d} C_4^{u,d} = 2m_s \text{Im} (C_g^{R,L}), \quad (43)$$

where one should replace  $\lambda_{iq}^{AB} = V_{iq}^{*A} V_{iq}^B$ , thus selecting in Eq. (24) only the LR terms.

The Wilson coefficient of the three-gluon operator  $\mathcal{O}_5$  is suppressed by  $\alpha_s/4\pi$  and its contribution to the nEDM is negligible for light quarks. At the integration scale of each heavy quark it is given by [85–88]

$$C_5(m_q) = \frac{\alpha_s(m_q)}{8\pi} C_4^q(m_q), \quad (44)$$

with  $q = b$  giving the dominant contribution, proportional to  $m_t/m_b$  (see Eq. (24)).

By inspection of Eqs. (22)–(24), the leading operators induced by gauge boson exchange, which are sensitive to the new CP phases through the LR mixing  $\zeta$ , are those obtained from  $Q_2^{LR,RL}$  and  $Q_{g,\gamma}^{L,R}$ . The  $\mathcal{O}_{1,2}^q$  operators are induced by neutral scalar exchange with CP-violating couplings ( $Z$  boson exchange does not induce CP violating transitions). On the other hand, the contributions of the heavy doublet Higgs, that we assume decoupled at a scale higher than the right-handed gauge bosons, are always suppressed by the light quarks Yukawa couplings, and are henceforth neglected. Analogously, the operators  $\mathcal{O}_{3,4}^{q'q}$  are not generated at the tree level in the model. They are obtained via gluonic corrections of  $\mathcal{O}_{1,2}^{q'q}$ . Since  $\mathcal{O}_{3,4}^{q'q}$  are flavor symmetric their contribution to the renormalization of  $\mathcal{O}_{1,2}^q$  and  $\mathcal{O}_{3,4}^q$  is proportional

to  $C_{1,2}^{q'q} + C_{1,2}^{qq'}$ , which vanishes to great accuracy in the present framework. One noticeable consequence is that the leading additive QCD renormalization of the dipole operators  $\mathcal{O}_{3,4}^q$  comes at the NLO in the loop expansion (LO in  $\alpha_s$ ) from the  $\mathcal{O}_{1,2}^{q'q}$  operators, in analogy to the  $\Delta S = 1$  case.

The QCD anomalous dimensions and mixings of the whole set of operators in Eq. (33), at the leading order in the loop expansion, are found in Ref. [85]. A more recent NLO calculation is presented in Ref. [89]. We report the relevant anomalous dimension matrix in Appendix C in our normalization. At the hadronic scale the Wilson coefficients  $C_1^{qq'}$  and  $C_2^{qq'}$  turn out to be comparable, with a slight predominance of the radiatively induced  $C_1^{qq'}$ .

The quark EDM from  $\mathcal{O}_3^q$  is given in units of  $e$  by

$$d_q = -\frac{G_F}{\sqrt{2}} \frac{e_q m_q}{4\pi^2} C_3^q \quad (45)$$

and analogously for the chromo-EDM

$$\tilde{d}_q = -\frac{G_F}{\sqrt{2}} \frac{m_q}{4\pi^2} C_4^q. \quad (46)$$

The neutron EDM can be obtained from Eqs. (45)–(46), evaluated at the hadronic scale, via naive dimensional analysis, chiral perturbation theory or QCD sum rules, the latter providing a more systematic approach. A recent reevaluation in the sum rule framework gives [90]

$$d_n/e \simeq 0.32d_d - 0.08d_u + 0.12\tilde{d}_d - 0.12\tilde{d}_u - 0.006\tilde{d}_s. \quad (47)$$

The contribution from the  $\bar{\theta}$  term is estimated as [91]

$$d_n \simeq -(0.9-1.2) \times 10^{-16} \bar{\theta} \quad (48)$$

in units of  $e \cdot \text{cm}$ . Due to the presence in Eq. (33) of effective CP and chiral-symmetry breaking operators a nonzero  $\bar{\theta}$  is induced even in the presence of a PQ axion [82, 92], as explicitly derived in Eq. (D19).

The contribution of the Weinberg three-gluon operator to the nEDM is subject to large hadronic uncertainties, related to the method of evaluation. By comparing different calculations one finds [93]

$$d_n = -(10-30 \text{ MeV}) \frac{G_F}{\sqrt{2}} \frac{eg_s}{8\pi^2} C_5(1 \text{ GeV}). \quad (49)$$

In the LR framework the dominant chirality flip of the dipole operators depends on the fermion masses in the loop. Albeit chirally unsuppressed, the two-loop Weinberg operator  $\mathcal{O}_5$  turns out to give a subleading contribution to the nEDM.

### C. The long-distance contributions

The operator  $\mathcal{O}_1^{qq'}$  mediates meson to vacuum transitions that when chirally rotated away generate CP-violating

interactions among mesons and baryons. These couplings induce via chiral loops potentially large contributions to the nEDM [83, 94]. As shown in Ref. [38], the pion VEV carries an enhancement factor  $m_s/(m_u + m_d)$  in specific meson-baryon couplings that leads the chiral loop contributions to the nEDM. As a matter of fact, by considering the  $U(3)_L \times U(3)_R$  chiral Lagrangian (Appendix D) with the inclusion of the axial anomaly term [95] one obtains

$$\langle \pi^0 \rangle \simeq \frac{G_F}{\sqrt{2}} (\mathcal{C}_{1ud} - \mathcal{C}_{1du}) \frac{4c_3}{B_0 F_\pi (m_d + m_u)}, \quad (50)$$

with  $\langle \pi^0 \rangle \gg \langle \eta_{0.8} \rangle$  by a factor  $m_s/(m_d - m_u)$ . For the notation and estimate of chiral couplings and low energy constants (LEC) see Appendix D.

Given the leading role of  $\langle \pi^0 \rangle$ , the relevant CP violating baryon-meson couplings are (see Eqs. (D16)–(D17))

$$\bar{g}_{np\pi} \simeq \frac{\sqrt{2}B_0}{F_\pi^2} (b_D + b_F)(m_d - m_u) \langle \pi^0 \rangle, \quad (51)$$

$$\bar{g}_{n\Sigma^- K^+} \simeq -\frac{B_0}{\sqrt{2}F_\pi^2} (b_D - b_F) m_s \langle \pi^0 \rangle, \quad (52)$$

with  $b_D + b_F \simeq -0.14$  and  $b_D - b_F \simeq 0.28$  in units of  $\text{GeV}^{-1}$ , thus exhibiting the  $m_s/(m_d - m_u)$  enhancement of  $\bar{g}_{n\Sigma^- K^+}$  over  $\bar{g}_{np\pi}$ .

Up to unknown LECs (that give subleading contributions according to a naive dimensional estimate [38]) the nEDM computed from baryon-meson chiral loops leads to [96, 97]

$$d_n \simeq \frac{e}{8\pi^2 F_\pi} \frac{\bar{g}_{n\Sigma^- K^+}}{\sqrt{2}} (D - F) \left( \log \frac{m_K^2}{m_N^2} - \frac{\pi m_K}{2m_N} \right), \quad (53)$$

to be compared with the LO pion contribution [98]

$$d_n \simeq -\frac{e}{8\pi^2 F_\pi} \frac{\bar{g}_{np\pi}}{\sqrt{2}} (D + F) \left( \log \frac{m_\pi^2}{m_N^2} - \frac{\pi m_\pi}{2m_N} \right), \quad (54)$$

where at the leading order  $D + F \equiv g_A \simeq 1.3$  and  $D - F \simeq 0.3$ . In Ref. [99] large logarithmic corrections to the tree level result are computed leading to  $D + F \simeq 1$  and  $D - F \simeq 0.2$ . We include this spread within the hadronic uncertainty in our numerical analysis. In Eqs. (53)–(54) the extended-on-mass-shell prescription is applied to ensure a correct power counting [100].

In spite of the large pion log, the enhanced  $\bar{g}_{n\Sigma^- K^+}$  coupling makes Eq. (53) the leading one, even when NLO pion loop contributions are included [30, 98].

As we shall shortly see, Eq. (53) gives the dominant contribution to the nEDM.

## VI. NUMERICAL ANALYSIS

### A. Preliminaries

According to Eq. (26) and to the discussion of the LR hadronic matrix elements in Sect. IV B we obtain

$$h_{\varepsilon'} = 0.92 \times 10^6 |\zeta| \left[ \sin(\alpha - \theta_u - \theta_d) + \sin(\alpha - \theta_u - \theta_s) \right] \\ + 320 |\zeta| \left[ \sin(\alpha - \theta_c - \theta_d) + \sin(\alpha - \theta_c - \theta_s) \right] \\ + 6200 r \sin(\theta_d - \theta_s), \quad (55)$$

which is normalized to unity when matching the central experimental value in Eq. (30). The contributions that are proportional to the LR mixing  $\zeta$  in Eq. (3) are due to current-current (first line) and dipole operators (second line), while the term proportional to  $r$  represents the RR current contribution. The relative magnitude of the three contributions is readily estimated. From the direct search limit  $M_{W_R} \gtrsim 3.7 \text{ TeV}$  (see [33]) one obtains an upper bound on the mixing,  $\zeta < 4 \times 10^{-4}$ . Thus, the first line can easily overshoot by orders of magnitudes the experimental value. The contribution of the dipoles instead amounts at most to  $h_{\varepsilon'} \sim 0.25$ . As for the last line, the phase  $\theta_d - \theta_s$  is constrained by  $\varepsilon_K$ , with different outcomes in the  $\mathcal{C}$  or  $\mathcal{P}$  cases. In the case of  $\mathcal{C}$ , from Eq. (16) one finds  $r \sin(\theta_d - \theta_s) < 1.4 \times 10^{-4}$ , so that this contribution falls short of  $\sim 0.08$  and can be neglected. In the case of  $\mathcal{P}$ , from Eq. (17) one has  $\sin(\theta_d - \theta_s \pm 0.16) < (M_{W_R}/30 \text{ TeV})^2$  and it can contribute to  $h_{\varepsilon'}$  as much as 0.5. These maximal values are reduced for higher LR scale.

It is convenient to note that in the dominant contribution to  $\varepsilon'$ , namely

$$h_{\varepsilon'} \simeq 0.92 \times 10^6 |\zeta| \left[ \sin(\alpha - \theta_u - \theta_d) + \sin(\alpha - \theta_u - \theta_s) \right] \quad (56)$$

the relation between  $\theta_d$  and  $\theta_s$  Eqs. (16)–(17) enforced for low LR scale implies that the result depends effectively on a single combination of phases, e.g.  $\alpha - \theta_u - \theta_d$ .

Turning to the neutron electric dipole moment, in analogy with  $\varepsilon'$  it is convenient to introduce the parameter

$$h_{d_n} = \frac{d_n^{LR}}{d_n^<} , \quad (57)$$

where the LR contribution to the dipole moment is normalized to the present experimental bound,  $d_n^< = 2.9 \times 10^{-26} \text{ e cm}$ .

From the results of the previous section and those in the appendices we finally obtain for central values of the

parameters at the neutron scale

$$h_{d_n}^{\text{noPQ}} = 10^6 |\zeta| \left[ -1.74 \sin(\alpha - \theta_u - \theta_d) \right. \\ \left. - 0.014 \sin(\alpha - \theta_c - \theta_d) \right. \\ \left. + 0.00094 \sin(\alpha - \theta_t - \theta_b) \right], \quad (58)$$

$$h_{d_n}^{\text{PQ}} = 10^6 |\zeta| \left[ -2.63 \sin(\alpha - \theta_u - \theta_d) \right. \\ \left. - 0.010 \sin(\alpha - \theta_c - \theta_d) \right. \\ \left. + 0.00094 \sin(\alpha - \theta_t - \theta_b) \right], \quad (59)$$

where the first line includes the contribution of the LR current-current operators via chiral loops, and in the PQ case also via the induced shift on  $\bar{\theta}$ . We can see that the latter contributes one third of the result. The much smaller second and third lines derive from the dipole and the Weinberg operators respectively (including the renormalization mixing). The results are in fairly good agreement with those reported in Ref. [38].

In the discussion that follows we will consider these outcomes as benchmark values. In order to consider the uncertainties discussed in the previous sections, we allow a range of 50%–200% for  $h_{\varepsilon'}$  due mostly to the relevant LR matrix elements, and a 30% uncertainty on  $h_{d_n}$  related to the long-distance parameters  $D$  and  $F$  in Eqs. (53)–(54).

It appears immediately that the combinations of phases in the leading terms of Eq. (55) and Eqs. (58)–(59) can lead to correlations that open the possibility to test the LR setup. This is especially clear for low scale  $M_{W_R} < 30 \text{ TeV}$  because, in view of the  $\varepsilon$  constraints in Eqs. (16)–(17),  $\theta_d$  and  $\theta_s$  are strongly related.

In the following, we explore this correlation by considering the two phenomenological scenarios for  $\varepsilon'/\varepsilon$ : namely, whether the SM prediction falls short of the experimental value with the missing contribution being provided by low scale LRSM, or whether the SM prediction saturates the observable and thus a lower bound on the  $W_R$  mass follows.

It is then crucial to consider the difference between the  $\mathcal{P}$  and  $\mathcal{C}$  choice of the discrete LR symmetry. The important feature is that the phases  $\theta_i$  are free for  $\mathcal{C}$ , while for  $\mathcal{P}$  they are predicted as a function of  $s_\alpha t_{2\beta}$ . Therefore, in the case of  $\mathcal{C}$  one can always suppress the effects CP violation by setting the phases to zero, and thus no lower bound can be placed on the  $W_R$  scale. On the contrary, requiring a sizeable contribution to  $\varepsilon'$  bounds the size LR scale from above. For the case of  $\mathcal{P}$  the phases can be calculated analytically in a power series of  $s_\alpha t_{2\beta}$ , as demonstrated in [17]. For our purposes it is enough to consider the leading order expressions, which we recalculate for generic signs  $s_i$  (see Appendix A for the detailed expressions).

In summary, for the sake of clarity, we shall discuss our results with reference to two alternative scenarios in

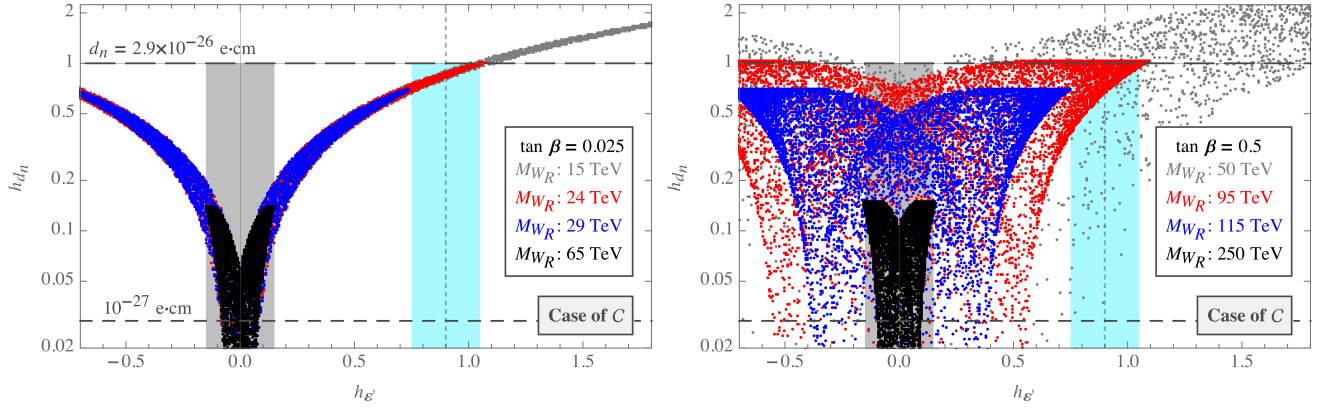


FIG. 1. Case of  $\mathcal{C}$ : Contribution of the LRSM to  $\varepsilon'$  and  $d_n$  for random phases, various choices of  $M_{W_R}$  and two choices of  $t_\beta$ : small  $t_\beta = m_b/m_t$  (left) or large  $t_\beta = 0.5$  (right). Only those points that satisfy the  $\varepsilon$  constraint are shown. The left (gray) and right (cyan) vertical bands define the  $\varepsilon'_{\text{SM}}$  and  $\varepsilon'_{\text{NP}}$  scenarios respectively. The long-dashed line represent the current  $d_n$  experimental bound and the short-dashed one a future reach of  $d_n < 10^{-27} e \cdot \text{cm}$ .

which i) the SM saturates the experimental value of  $\varepsilon'/\varepsilon$  and thus the LRSM contribution has to be bounded from above, or ii) the SM contribution falls within the present experimental error and the LRSM contribution provides about the whole amount. We name these limiting scenarios  $\varepsilon'_{\text{SM}}$  and  $\varepsilon'_{\text{NP}}$  respectively. In either case we require the contribution to  $d_n$  to be less than the present experimental bound (the effect of future experimental improvements are also shown). Thus, we set

$$\begin{aligned} \varepsilon'_{\text{SM}} : \quad & h_{d_n} < 1. \text{ and } |h_{\varepsilon'}| < 0.15, \\ \varepsilon'_{\text{NP}} : \quad & h_{d_n} < 1. \text{ and } h_{\varepsilon'} = 0.9 \pm 0.15. \end{aligned}$$

The uncertainty of 0.15 is related to the present experimental error on  $\varepsilon'/\varepsilon$ .

An illustration of the predictions for  $h_{\varepsilon'}$  and  $h_{d_n}$  is given as a scatter plot in Figs. (1) and (2), for the cases of  $\mathcal{C}$  and  $\mathcal{P}$  respectively, for different values of the model parameters. The studied  $\varepsilon'_{\text{SM}}$  and  $\varepsilon'_{\text{NP}}$  scenarios are depicted by the left (gray) and right (cyan) vertical bands respectively.

## B. Results

Our results are summarized in figures (1) to (5). We analyze separately the  $\mathcal{C}$  and  $\mathcal{P}$  cases.

**Case of  $\mathcal{C}$ .** Because the phases are free parameters, the LRSM contribution to both  $\varepsilon'$  and  $d_n$  can be made vanishing by appropriate tuning. Correspondingly, in Fig. 1 the dots populate the gray band no matter how low  $M_{W_R}$  is; as a result, no bound on  $M_{W_R}$  can be placed in the  $\varepsilon'_{\text{SM}}$  scenario.

In the  $\varepsilon'_{\text{NP}}$  scenario instead, because one requires a sizeable contribution of the LRSM to  $\varepsilon'$ , an upper bound on  $M_{W_R}$  appears. Its size clearly depends on  $t_\beta$ . For instance, for large  $t_\beta \simeq 0.5$ , near its perturbativity limit (right frame in Fig. 1), one sees that  $W_R$  must be lighter

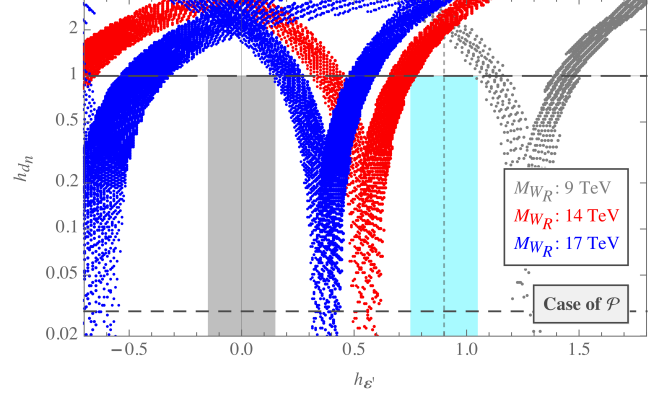


FIG. 2. Case of  $\mathcal{P}$ : Contribution of the LRSM to  $\varepsilon'$  and  $d_n$  for various choices of  $M_{W_R}$  by scanning on phases and  $t_\beta$ , while satisfying the  $\varepsilon$  constraint. The left (gray) and right (cyan) vertical bands define the  $\varepsilon'_{\text{SM}}$  and  $\varepsilon'_{\text{NP}}$  scenarios respectively. The long-dashed line denotes the current experimental upper bound, while the short-dashed one a future reach of  $d_n < 10^{-27} e \cdot \text{cm}$ .

than 115 TeV, while for  $t_\beta = 0.025$ ,  $W_R < 30$  TeV is required (left frame).

One also notices that the correlation between  $\varepsilon'$  and  $d_n$  is sharper for  $W_R$  lighter than  $\sim 30$  TeV (left frame). In this regime due to the  $\varepsilon_K$  constraint  $\theta_s - \theta_d$  has to be small (modulo  $\pi$ ). Then the dominant first lines in Eq. (58) and Eq. (55) depend on the same phase combination and are thus confined in a tiny strip (left frame). This correlation is progressively absent in the large  $t_\beta$  regime (right frame) because there  $W_R$  is much heavier and the  $\varepsilon$  constraint becomes less effective.

In any case, since the free phases as well as  $\alpha$  are at present not directly tested by other observations, it is convenient to marginalize over them and show the resulting upper bound on  $M_{W_R}$  correlated with  $t_\beta$ . This is depicted in Fig. 3, where the upper bound on  $M_{W_R}$  in

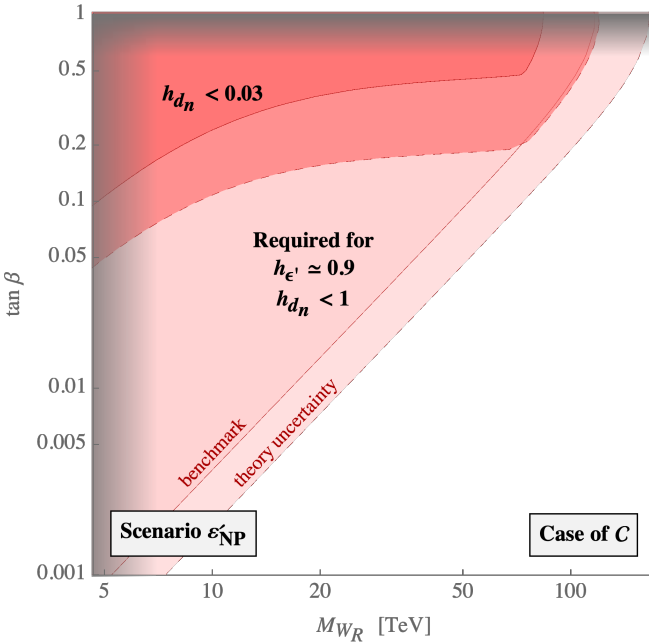


FIG. 3. Case of  $\mathcal{C}$  in  $\epsilon'_{\text{NP}}$  scenario: Allowed region in the  $M_{W_R}$ – $\tan\beta$  plane for 0.9  $\epsilon'_{\text{exp}}$  to arise from new physics. The nEDM prediction is taken below 1 (light shading) or 0.03 (dark shading) of the present experimental bound. Solid lines correspond to the chosen benchmark values of the hadronic parameters, while the dashed contours include the theoretical uncertainty. In the progressively shaded band at the top,  $\tan\beta \gtrsim 0.6$ , quark Yukawa couplings become non-perturbative, while at the left, for  $M_{W_R} < 6$  TeV, the scalar sector becomes non-perturbative [31].

the  $\epsilon'_{\text{NP}}$  scenario is seen to range from less than 10 TeV (for  $\tan\beta \sim 10^{-3}$ ) up to 100 TeV (for maximal  $\tan\beta$ ).

In Fig. 3 we also show the effect of tightening the constraint on  $d_n$  to  $< 0.03$ , in view of the future experiments. One can conclude that when this bound will be reached, the LRSM contribution to  $\epsilon'$  can take place only for somewhat large  $\tan\beta \gtrsim 0.1$ .

We depict with a dashed contour the bound after including the theoretical uncertainties dominated by those on the matrix elements. A numerical difference can be appreciated, but the picture patterns remain.

**Case of  $\mathcal{P}$ .** In this case all phases are predicted in terms of  $\alpha$  and  $\tan\beta$ , and although the 32 different combinations of signs  $s_{u,c,t,d,s}$  (see Eq. (10)) give rise to different numerical predictions, the resulting picture illustrated in Fig. 2 shows well defined and narrow bands. One can observe that the new physics contribution to  $\epsilon'$  shows a different pattern with respect to the previous case.

First, for low scale  $W_R$  it is not possible to make  $\epsilon'$  vanishing by a convenient choice of phases, and thus a lower bound on  $M_{W_R}$  emerges in the  $\epsilon'_{\text{SM}}$  scenario. As anticipated above, the reason is the role played by the  $\epsilon_K$  constraint Eq. (17): for low scale  $W_R$  one must have quite a large  $\theta_s - \theta_d \sim \pm 0.16$  [25] and so the combinations in Eq. (55) can never vanish in correspondence of vanishing

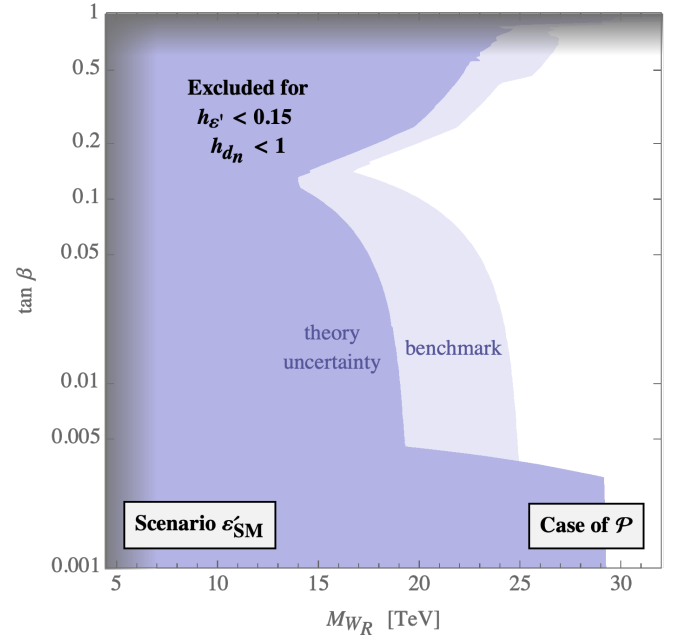


FIG. 4. Case of  $\mathcal{P}$ : The shaded regions in the  $M_{W_R}$ – $\tan\beta$  plane are excluded by the requirement of having at most a 15% new physics contribution to  $\epsilon'/\epsilon$  and  $d_n$  below the present experimental bound. The lighter region assumes benchmark values for the hadronic parameters, while the darker one includes the theory uncertainty, as discussed in the text.

$h_{\epsilon'}$ ,  $h_{d_n}$ . Thus, by lowering  $M_{W_R}$  the predicted values of  $h_{\epsilon'}$  shift to larger values, as shown in Fig. 2.

From the plot it can be argued that the  $\epsilon'_{\text{SM}}$  scenario requires  $M_{W_R} \gtrsim 16$  TeV. The detailed analysis gives information on the correlations between the phases and scales involved, as we report in appendix E, that shows the complex interplay of the 32 sign combinations and the tight correlation among  $\alpha$ ,  $\tan\beta$  and  $M_{W_R}$ .

With the numerical study at hand, by marginalizing on  $\alpha$  we depict in Fig. 4 the lower bound on  $M_{W_R}$  as a function of  $\tan\beta$ . We find that the lowest allowed scale  $M_{W_R} \gtrsim 16$  TeV is achieved for  $\tan\beta \sim 0.15$ . The darker area shows the impact of including the theory uncertainty dominated by the hadronic matrix elements (100% for  $\epsilon'$  and 30% for nEDM). This relaxes the lower bound to a least possible value of  $M_{W_R} \gtrsim 14$  TeV, which is achieved for  $\tan\beta \sim 0.1$ .

In the  $\epsilon'_{\text{NP}}$  scenario the situation is even more structured and interesting. The constraint  $h_{d_n} < 1$  can be satisfied by choosing the vacuum phase  $\alpha$  appropriately, if possible, thus providing a prediction of  $h_{\epsilon'}$ . As expected, the request  $h_{\epsilon'} \simeq 0.9 \pm 0.15$  sharply constrains the range of  $M_{W_R}$ . For instance in Fig. 2, for benchmark parameters, a preferred range of  $M_{W_R} = 9\text{--}14$  TeV emerges. This is better seen in Fig. 5 where by marginalizing again on  $\alpha$  we depict the allowed region in the plane  $M_{W_R}$ – $\tan\beta$  for the  $\epsilon'_{\text{NP}}$  scenario in the case of  $\mathcal{P}$  with benchmark hadronic parameters (darker shaded area). The region spans the interval  $\tan\beta \simeq 0.005\text{--}0.1$ . When we include the

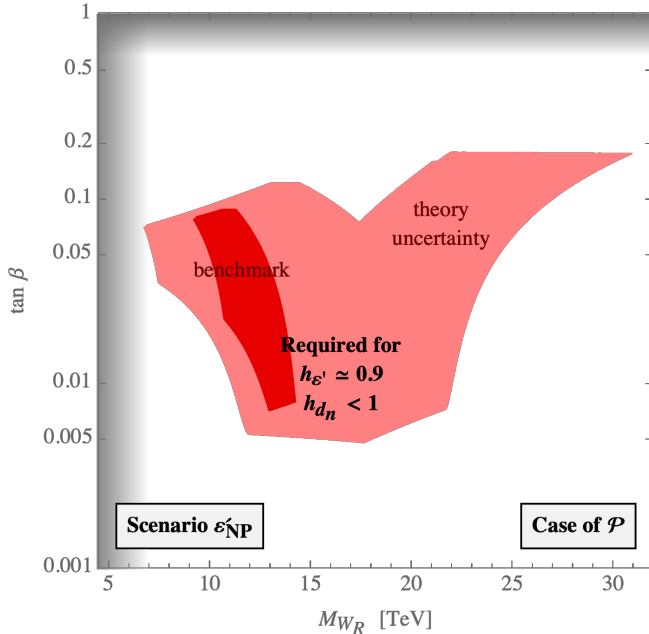


FIG. 5. Case of  $\mathcal{P}$ : The shaded regions in the  $M_{W_R} - t_\beta$  plane are allowed in order for new physics to provide  $0.9 \epsilon'_{\text{exp}}$ , while keeping the contribution to  $d_n$  below the present experimental bound. The smaller region assumes benchmark values for the hadronic parameters, while the larger one includes the theory uncertainties, as discussed in the text.

hadronic uncertainties (lighter shaded area) we find that the allowed region relaxes substantially in the  $M_{W_R}$  direction, which spans the 7–30 TeV interval.

In summary, in the case of  $\mathcal{P}$ , our numerical analysis shows that with conservative theoretical uncertainties the  $\epsilon'_{\text{SM}}$  scenario places a lower bound  $M_{W_R} \gtrsim 14$  TeV, while the  $\epsilon'_{\text{NP}}$  scenario requires  $M_{W_R} = 7$ –30 TeV and  $t_\beta = 0.005$ –0.2. Both these bounds will get considerably tighter with the expected reduction of the theoretical errors on  $\epsilon'$ , coming from a precise lattice determination of the relevant hadronic matrix elements.

## VII. CONCLUSIONS

In this work we have revisited the CP-violating observables  $\epsilon$ ,  $\epsilon'$  and  $d_n$  within the LRSM and derived updated limits on the LR scale  $M_{W_R}$  and model parameters. In particular, our analysis aimed to fully investigate the correlations among the observables for the different setups of the model parameters, arising by a given choice of discrete LR symmetry.

The issue is relevant also in the light of the recently reopened debate on the magnitude of the theoretical SM prediction for  $\epsilon'$  following the recent lattice results, suggesting that the SM may fall short of reproducing the experimental value of  $\epsilon'/\epsilon$ . While waiting for a fully consistent picture of the kaon hadronic decays from lat-

tice, we considered here two limiting scenarios named as  $\epsilon'_{\text{SM}}$  and  $\epsilon'_{\text{NP}}$  respectively, according to whether the SM or the LRSM saturate the experimental value.

In the LRSM each choice of  $\mathcal{P}$  or  $\mathcal{C}$  discrete symmetry implies crucially different predictions and constraints for the RH CKM phases with a strong impact on the new physics scale.

Previous detailed studies on  $\epsilon, \epsilon'$  in the LRSM can be found in [23–25], and of  $\epsilon, \epsilon', d_n$  in [30, 38]. In particular, the LRSM prediction for  $\epsilon$  was thoroughly analyzed in [25] and gives a tight constraint on the RH CKM phases versus the LR scale. On the other hand the relation with  $d_n$  was studied recently in [30] mainly within the assumption of exact  $\mathcal{P}$  parity and thus with vanishing QCD theta term (although the possibility of a different UV completion was foreseen).

In order to offer a predictive scenario for the neutron dipole moment, we invoke the PQ setup as a dynamical solution of the theta QCD problem and investigate the impact of its explicit breaking by the effective operators in the minimal LRSM. The analysis shows that while this adds a new contribution to  $d_n$  from the shift of the axion field, just a minor numerical difference results in the outcomes. Another difference of the present work with respect of [30] is that the weak contributions to  $d_n$  are evaluated with  $SU(3)$  chiral symmetry [38], that shows that the strange quark contribution turns out to be dominant in the chiral loops.

More recent studies on this topic appeared in the literature. In particular i) in [37] the authors address the RH interactions in an effective parametrization, ii) in [38] the authors address the LRSM model with  $\mathcal{C}$  symmetry, seemingly ignoring the phase correlations deriving from the  $\epsilon$  constraint, and focusing on small  $t_\beta$  only; iii) in [39] the case of  $\mathcal{P}$  symmetry is analyzed by decoupling the scale of LR gauge interactions,  $M_{W_R}$ , and effectively studying a two Higgs doublet model. The study presented here aims to provide a comparative picture of the implications of  $\epsilon, \epsilon'$  and  $d_n$  on the minimal LRSM setups, exhibiting the main patterns of the observable correlations on the model parameters and scales.

Our conclusions in the  $\epsilon'_{\text{SM}}$  scenario can be summarized as follows: for the choice of  $\mathcal{C}$  symmetry, which allows for several free phases, one finds constraints on them but no lower bound on the RH scale is present. For the choice of  $\mathcal{P}$  instead, where the CKM phases are predicted in terms of one vacuum phase, we find a bound  $M_{W_R} > 14$  TeV, including conservative theoretical uncertainties on the hadronic parameters. Future improvement on these uncertainties will push this bound slightly higher to 17 TeV. This is in any case smaller than the tight lower bound of  $\sim 30$  TeV which stems from exact parity  $\mathcal{P}$  [30].

In the  $\epsilon'_{\text{NP}}$  scenario, the LRSM contributions may saturate  $\epsilon'$  and still hold the  $d_n$  below the experimental bound or at the reach of future probes. An upper limit on  $M_{W_R}$  is naturally demanded for this to happen. The

case of  $\mathcal{P}$ , being more constrained, requires  $M_{W_R} = 8$ –30 TeV (or  $M_{W_R} = 9$ –13 TeV with benchmark hadronic parameters) and  $t_\beta \sim 0.01$ –0.1. On the other hand for the  $\mathcal{C}$  case, the LR contributions can saturate  $\varepsilon'$  for  $M_{W_R}$  as large as 100 TeV with increasingly large  $\theta_\beta$ , from 0.001 to its perturbativity bound  $\simeq 0.5$ .

The scale of  $M_{W_R} \sim 10$  TeV lies just beyond the reach of LHC in the golden KS channel [33]. On the other hand, it may show up as an effective interaction either in the dilepton channel or, for a particular range of neutrino masses, in displaced decays of Higgs to two RH neutrinos [101]. A future hadronic collider at 30 TeV center-of-mass energy would probe naturally this mass scale both in the KS process [102] or lepton plus missing energy channel [33].

$$\theta_u + \theta_d \simeq \frac{s_\alpha t_{2\beta}}{2} \left[ \sin^2 \theta_{12} \left( \frac{2s_s}{m_s} - \frac{s_d}{m_d} \right) (m_c s_c \cos^2 \theta_{23} + m_t s_t \sin^2 \theta_{23}) - \frac{s_u}{m_u} (m_d s_d \cos^2 \theta_{12} + s_s m_s \sin^2 \theta_{12}) \right] + \frac{s_u - s_d}{2} \pi, \quad (\text{A1})$$

$$\theta_u + \theta_s \simeq \frac{s_\alpha t_{2\beta}}{2} \left[ \cos^2 \theta_{12} \frac{s_s}{m_s} (m_c s_c \cos^2 \theta_{23} + m_t s_t \sin^2 \theta_{23}) - \frac{s_u}{m_u} (m_d s_d \cos^2 \theta_{12} + m_s s_s \sin^2 \theta_{12}) \right] + \frac{s_u - s_s}{2} \pi. \quad (\text{A2})$$

## Appendix B: Loop functions

The loop functions relevant for the SM and the LRSM short-distance coefficients in Eqs. (22)–(24) are [21, 103–105]

$$F_1^{LL} = \frac{x(-18 + 11x + x^2)}{12(x-1)^3} - \frac{(4 - 16x + 9x^2) \ln x}{6(x-1)^4} \quad (\text{B1})$$

$$E_1^{LL} = -\frac{x^2(5x^2 - 2x - 6)}{18(x-1)^4} \ln x + \frac{19x^3 - 25x^2}{36(x-1)^3} + \frac{4}{9} \ln x \quad (\text{B2})$$

$$F_2^{LL} = \frac{x(2 + 3x - 6x^2 + x^3 + 6x \ln x)}{4(x-1)^4} \quad (\text{B3})$$

$$E_2^{LL} = \frac{x(8x^2 + 5x - 7)}{12(x-1)^3} + \frac{x^2(2 - 3x)}{2(x-1)^4} \ln x \quad (\text{B4})$$

$$F_2^{LR} = \frac{-4 + 3x + x^3 - 6x \ln x}{2(x-1)^3}, \quad (\text{B5})$$

$$E_2^{LR} = \frac{5x^2 - 31x + 20}{6(x-1)^2} - \frac{x(2 - 3x)}{(x-1)^3} \ln x. \quad (\text{B6})$$

In addition, one has  $F_{1,2}^{RR} = F_{1,2}^{LL}(rx_i)$  and similarly for  $E_{1,2}^{RR}$ .

## Appendix C: Anomalous dimensions

As explained in Sect. V the pattern of model values of the weak scale Wilson coefficients in Eq. (33) allow us to

## ACKNOWLEDGMENTS

We thank Goran Senjanović for interesting discussions. AM was partially supported by the Croatian Science Foundation project number 4418.

## Appendix A: The external phases of $V_R$

In the case of  $\mathcal{P}$  the external phases can be worked out from the perturbatively computed  $V_R$  [40] in Eq. (9). For the analysis on  $d_n$  and  $\varepsilon'$  performed in this article, the relevant phase combinations are  $\theta_u + \theta_d$  and  $\theta_u + \theta_s$ , that can be expressed in terms of the quark masses, the CKM angles, the expansion parameter  $s_\alpha t_{2\beta}$  and the arbitrary signs  $s_i$ :

reduce the basis of the effective operators to

$$\mathcal{O}_{qq'} = \{\mathcal{O}_1^{qq'}, \mathcal{O}_2^{qq'}, \mathcal{O}_1^{q'q}, \mathcal{O}_2^{q'q}\}, \quad (\text{C1})$$

$$\mathcal{O}_q = \{\mathcal{O}_3^q, \mathcal{O}_4^q\}. \quad (\text{C2})$$

The LO mixing matrix of the  $\mathcal{O}_{qq'}$  operators is given by [85]

$$\gamma_{qq' \rightarrow qq'}^{(1)} = \begin{pmatrix} -16 & 0 & 0 & 0 \\ -6 & 2 & 0 & 0 \\ 0 & 0 & -16 & 0 \\ 0 & 0 & -6 & 2 \end{pmatrix} \quad (\text{C3})$$

while the dipole anomalous-dimension matrix (we neglect the mixing of  $\mathcal{O}_5$  into  $\mathcal{O}_4^q$ ) reads [106, 107]

$$\gamma_{q \rightarrow q}^{(1)} = \begin{pmatrix} \frac{32}{3} & 0 \\ \frac{32}{3} & \frac{28}{3} \end{pmatrix} \quad (\text{C4})$$

The subscripts  $qq'$  and  $q$  in the  $\gamma$ 's indicate the non-vanishing subblocks of the anomalous-dimension matrix.

The mixing of  $\mathcal{O}_{qq'}$  into the dipoles is readily obtained from Ref. [89], taking into account the different operator basis and the covariant derivative conventions

$$\gamma_{qq' \rightarrow q}^{(1)} = \begin{pmatrix} \frac{8}{3} \frac{e_{q'}}{e_q} \frac{m_{q'}}{m_q} & -\frac{67}{6} \frac{m_{q'}}{m_q} \\ -8 \frac{e_{q'}}{e_q} \frac{m_{q'}}{m_q} & -\frac{5}{2} \frac{m_{q'}}{m_q} \\ \frac{8}{9} \frac{e_{q'}}{e_q} \frac{m_{q'}}{m_q} & -\frac{67}{18} \frac{m_{q'}}{m_q} \\ -\frac{8}{3} \frac{e_{q'}}{e_q} \frac{m_{q'}}{m_q} & -\frac{5}{6} \frac{m_{q'}}{m_q} \end{pmatrix}. \quad (\text{C5})$$

The Wilson coefficients evolve according to

$$\frac{dC}{d \log \mu} = C \gamma^{(1)} \frac{\alpha_s}{4\pi}, \quad (\text{C6})$$

where  $\gamma^{(1)}$  is the  $6 \times 6$  anomalous dimension matrix. The  $\gamma$ 's superscript indicates the  $\alpha_s/4\pi$  order of the mixing.

The short-distance running of the LR effective operators for  $\Delta S = 1$  and  $\Delta S = 2$  transitions is discussed in Refs. [23, 25], respectively.

#### Appendix D: The meson and baryon chiral Lagrangians

The LO chiral Lagrangian for the octet of Nambu-Goldstone bosons and the  $\eta_0$  singlet, including the bosonic representation of the  $\mathcal{O}_{1q'q}$  operator is given by

$$\begin{aligned} \mathcal{L} = & \frac{F_\pi^2}{4} \text{tr} [(D_\mu U)^\dagger D^\mu U + \chi(U + U^\dagger)] \\ & + a_0 \text{tr} [\log U - \log U^\dagger]^2 \\ & + \frac{G_F}{\sqrt{2}} \sum_{u,d,s} \{ i \mathcal{C}_{ijkl}^{LRLR} (c_1 [U]_{ji} [U]_{lk} - c_1 [U^\dagger]_{ji} [U^\dagger]_{lk} \\ & + c_2 [U]_{li} [U]_{jk} - c_2 [U^\dagger]_{li} [U^\dagger]_{jk}) \\ & + i \mathcal{C}_{ijkl}^{RLLR} (c_3 [U^\dagger]_{ji} [U]_{lk} - c_3 [U]_{ji} [U^\dagger]_{lk}) \}, \quad (\text{D1}) \end{aligned}$$

where we follow the notation of Ref. [38]. The  $3 \times 3$  matrix  $U$  represents nonlinearly the nine Goldstone states. Under  $U(3)_L \times U(3)_R$  rotations  $L \times R$  it transforms as  $U \rightarrow RUL^\dagger$ , while  $\chi$  includes explicitly the quark masses, namely

$$U = \exp \left[ \frac{2i}{\sqrt{6}F_0} \eta_0 I + \frac{2i}{F_\pi} \Pi \right], \quad (\text{D2})$$

$$\Pi \equiv \begin{pmatrix} \frac{1}{2}\pi^0 + \frac{1}{2\sqrt{3}}\eta_8 & \frac{1}{\sqrt{2}}\pi^+ & \frac{1}{\sqrt{2}}K^+ \\ \frac{1}{\sqrt{2}}\pi^- & -\frac{1}{2}\pi^0 + \frac{1}{2\sqrt{3}}\eta_8 & \frac{1}{\sqrt{2}}K^0 \\ \frac{1}{\sqrt{2}}K^- & \frac{1}{\sqrt{2}}\bar{K}^0 & -\frac{1}{\sqrt{3}}\eta_8 \end{pmatrix}, \quad (\text{D3})$$

$$\chi = 2B_0 \text{diag}\{m_u, m_d, m_s\}, \quad (\text{D4})$$

and  $I$  is the identity matrix.  $F_\pi$  is the pion decay constant in the chiral limit, while  $F_0$  denotes the  $\eta_0$  decay constant, which we approximate to be equal. The quark mass term is written in terms of the condensate  $B_0 \simeq m_\pi^2/(m_u + m_d)$ .

The second term in Eq. (D1) represents the anomaly induced by the QCD instantons in the large  $N$  limit [95]. The coupling  $a_0$  satisfies  $48a_0/F_0^2 \simeq m_\eta^2 + m_{\eta'}^2 - 2m_K^2$ .

The third term represents the bosonization of  $\mathcal{C}_{1q'q} \mathcal{O}_{1q'q}$  where the sum over  $q \neq q' = u, d, s$  is understood. The coefficients that encode the short distance physics are given by  $\mathcal{C}_{ijkl}^{LRLR} = \mathcal{C}_{ijkl}^{RLLR} \equiv$

$\sum_{q \neq q'} \mathcal{C}_{1q'q} \delta_{iq'} \delta_{jq'} \delta_{kq} \delta_{lq}$ . The unknown low energy constants (LEC)  $c_{1,2,3}$ , are estimated in the large  $N$  limit as

$$c_1 \sim c_2 \sim c_3 \sim \frac{F_\pi^4 B_0^2}{4}. \quad (\text{D5})$$

The terms proportional to  $c_1$  and  $c_3$  induce VEVs of the Goldstone nonet. However, the  $c_1$  terms are proportional to  $(\mathcal{C}_{1ud} + \mathcal{C}_{1du})$ , which vanishes due to Eq. (41). Thus, only the  $c_3$  contributions, proportional to  $(\mathcal{C}_{1ud} - \mathcal{C}_{1du})$  are non vanishing. By neglecting  $|\mathcal{C}_{1qs}|$  ( $q = u, d$ ) with respect to  $|\mathcal{C}_{1ud}|$  we confirm the results in [38]

$$\begin{aligned} \langle \pi^0 \rangle \simeq & \frac{G_F}{\sqrt{2}} (\mathcal{C}_{1ud} - \mathcal{C}_{1du}) \frac{c_3}{B_0 F_\pi^2} \\ & \times \frac{B_0 F_\pi^2 (m_u + m_d) m_s + 8a_0 (m_u + m_d + 4m_s)}{B_0 F_\pi^2 m_u m_d m_s + 8a_0 (m_u m_d + m_d m_s + m_s m_u)}, \end{aligned} \quad (\text{D6})$$

$$\begin{aligned} \langle \eta_8 \rangle \simeq & \frac{G_F}{\sqrt{2}} (\mathcal{C}_{1ud} - \mathcal{C}_{1du}) \frac{c_3}{\sqrt{3} B_0 F_\pi^2} (m_d - m_u) \\ & \times \frac{B_0 F_\pi^2 m_s + 24a_0}{B_0 F_\pi^2 m_u m_d m_s + 8a_0 (m_u m_d + m_d m_s + m_s m_u)}, \end{aligned} \quad (\text{D7})$$

$$\begin{aligned} \langle \eta_0 \rangle \simeq & \frac{G_F}{\sqrt{2}} (\mathcal{C}_{1ud} - \mathcal{C}_{1du}) \frac{\sqrt{2}c_3}{\sqrt{3} B_0 F_\pi^2} (m_d - m_u) \\ & \times \frac{B_0 F_\pi^2 m_s}{B_0 F_\pi^2 m_u m_d m_s + 8a_0 (m_u m_d + m_d m_s + m_s m_u)}, \end{aligned} \quad (\text{D8})$$

where the leading short distance coefficients  $\mathcal{C}_{1qq'}$  are given in Eq. (41). The comparison of Eqs. (D6)–(D8) show the  $m_s/(m_d - m_u)$  enhancement of  $\langle \pi^0 \rangle$  over the others (empirically  $20a_0 \simeq B_0 F_\pi^2 m_s$ ).

The relevant baryon chiral Lagrangian can be written as [95]

$$\begin{aligned} \mathcal{L}_B = & \text{Tr} [\bar{B} i \gamma^\mu (\partial_\mu B + [\Gamma_\mu, B]) - M_B \bar{B} B] \\ & - \frac{D}{2} \text{tr} [\bar{B} \gamma^\mu \gamma_5 \{\xi_\mu, B\}] - \frac{F}{2} \text{tr} [\bar{B} \gamma^\mu \gamma_5 [\xi_\mu, B]] \\ & - \frac{\lambda}{2} \text{tr} [\xi_\mu] \text{tr} [\bar{B} \gamma^\mu \gamma_5 B] \\ & + b_D \text{tr} [\bar{B} \{\chi_+, B\}] + b_F \text{tr} [\bar{B} [\chi_+, B]] \\ & + b_0 \text{tr} [\chi_+] \text{tr} [\bar{B} B] + \dots, \end{aligned} \quad (\text{D9})$$

where

$$B = \begin{pmatrix} \frac{1}{\sqrt{2}}\Sigma^0 + \frac{1}{\sqrt{6}}\Lambda^0 & \Sigma^+ & p \\ \Sigma^- & -\frac{1}{\sqrt{2}}\Sigma^0 + \frac{1}{\sqrt{6}}\Lambda^0 & n \\ \Xi^- & \Xi^0 & -\frac{2}{\sqrt{6}}\Lambda^0 \end{pmatrix}, \quad (\text{D10})$$

$$U = \xi_R \xi_L^\dagger \quad (\xi_R = \xi_L^\dagger) \quad (\text{D11})$$

and

$$\Gamma_\mu \equiv \frac{1}{2}\xi_R^\dagger(\partial_\mu - i r_\mu)\xi_R + \frac{1}{2}\xi_L^\dagger(\partial_\mu - i l_\mu)\xi_L, \quad (\text{D12})$$

$$\xi_\mu \equiv i\xi_R^\dagger(\partial_\mu - i r_\mu)\xi_R - i\xi_L^\dagger(\partial_\mu - i l_\mu)\xi_L, \quad (\text{D13})$$

$$\chi_+ \equiv \xi_L^\dagger\chi\xi_R + \xi_R^\dagger\chi\xi_L. \quad (\text{D14})$$

Finally,  $M_B$  denotes the baryon mass in the chiral limit. In Eq. (D9) the interaction terms proportional to  $D$ ,  $F$  and  $\lambda$  are CP conserving, while those proportional to  $b_D$ ,  $b_F$  and  $b_0$  violate CP. The constants  $D$  and  $F$  are extracted from baryon semi-leptonic decays to be at tree level  $D \simeq 0.8$  and  $F \simeq 0.5$  [108], while from baryon mass splittings one obtains  $b_D \simeq 0.07 \text{ GeV}^{-1}$  and  $b_F \simeq -0.21 \text{ GeV}^{-1}$  [95].

By inserting  $\langle\pi^0\rangle$ ,  $\langle\eta_8\rangle$ ,  $\langle\eta_0\rangle$  into Eq. (D9) we can extract the relevant CP-violating interaction terms. Considering the vertices with one neutron and charged particles one obtains

$$\bar{g}_{np\pi} = \frac{B_0}{F_\pi}(b_D + b_F) \left[ \sqrt{2}(m_d - m_u) \frac{\langle\pi^0\rangle}{F_\pi} \right. \quad (\text{D15})$$

$$\left. - \frac{2\sqrt{2}}{\sqrt{3}}(m_u + m_d) \left( \frac{\langle\eta_8\rangle}{F_\pi} + \sqrt{2} \frac{\langle\eta_0\rangle}{F_0} \right) \right],$$

$$\bar{g}_{n\Sigma^-K^+} = \frac{B_0}{F_\pi}(b_D - b_F) \left[ -\frac{1}{\sqrt{2}}(3m_u + m_s) \frac{\langle\pi^0\rangle}{F_\pi} \right. \quad (\text{D16})$$

$$\left. - \frac{1}{\sqrt{6}}(m_u - 5m_s) \frac{\langle\eta_8\rangle}{F_\pi} - \frac{4}{\sqrt{3}}(m_u + m_s) \frac{\langle\eta_0\rangle}{F_0} \right],$$

which exhibit the enhancement of  $\bar{g}_{n\Sigma^-K^+}$  over  $\bar{g}_{np\pi}$  by a factor of order  $m_s/(m_d - m_u)$ .

When the LR scenario is endowed with a Peccei-Quinn symmetry the topological  $\theta$ -term can be rotated away by an appropriate axion dependent chiral rotation of the quark fields

$$q_L \rightarrow e^{-i\alpha_q/2}q_L, \quad q_R \rightarrow e^{i\alpha_q/2}q_R, \quad (\text{D17})$$

where  $\alpha_q$  depend on the axion field  $a$  as

$$\begin{aligned} \alpha_u &= \frac{m_d m_s}{m_u m_d + m_d m_s + m_s m_u} \left( \frac{a}{f_a} + \bar{\theta} \right), \\ \alpha_d &= \frac{m_s m_u}{m_u m_d + m_d m_s + m_s m_u} \left( \frac{a}{f_a} + \bar{\theta} \right), \\ \alpha_s &= \frac{m_u m_d}{m_u m_d + m_d m_s + m_s m_u} \left( \frac{a}{f_a} + \bar{\theta} \right), \end{aligned} \quad (\text{D18})$$

and  $f_a$  denotes the axion decay constant. With the chosen  $\alpha_q$  the axion does not mix with  $\pi^0$  and  $\eta_8$ . By applying such an  $U(3)_A$  field transformation to Eq. (D1), the axion field is included in the meson Lagrangian.

When only the leading  $(\mathcal{C}_{1ud} - \mathcal{C}_{1du})$  term is kept, the

vacuum is readily obtained as

$$\begin{aligned} \frac{\langle\pi^0\rangle}{F_\pi} &\simeq \frac{G_F}{\sqrt{2}}(\mathcal{C}_{1ud} - \mathcal{C}_{1du}) \frac{c_3}{B_0 F_\pi^2} \frac{m_u + m_d + 4m_s}{m_u m_d + m_d m_s + m_s m_u}, \\ \frac{\langle\eta_8\rangle}{F_\pi} &\simeq \frac{G_F}{\sqrt{2}}(\mathcal{C}_{1ud} - \mathcal{C}_{1du}) \frac{\sqrt{3}c_3}{B_0 F_\pi^2} \frac{m_d - m_u}{m_u m_d + m_d m_s + m_s m_u}, \\ \frac{\langle a \rangle}{f_a} + \bar{\theta} &\simeq \frac{G_F}{\sqrt{2}}(\mathcal{C}_{1ud} - \mathcal{C}_{1du}) \frac{2c_3}{B_0 F_\pi^2} \frac{m_d - m_u}{m_u m_d}. \end{aligned} \quad (\text{D19})$$

Due to the presence of CP and chiral breaking effective LR operators, the axion VEV no longer cancels the original  $\bar{\theta}$  term, leaving a calculable  $\bar{\theta}$  (Eq. (D19)) that contributes to the neutron EDM via Eq. (48). The meson VEVs above follow the pattern of Eqs. (D6)–(D7), with  $\langle\eta_0\rangle = 0$ .

In passing, let us note that also the axion mass is modified with respect to the standard result by the presence of the new CP and chiral breaking operators, but the deviation turns out to be utterly small.

## Appendix E: Numerical analysis for the case of $\mathcal{P}$

For the case  $\mathcal{P}$  there are 32 sign combinations  $\{s_u, s_c, s_t, s_d, s_s\}$ , corresponding to any choice of them being  $\pm 1$ , after having conventionally set  $s_b = 1$ . They give rise to different predictions for the  $V_R$  phases  $\theta_i$ , as shown e.g. in appendix A. As a consequence, the numerical analysis has to be repeated separately for each combination of signs.

For the  $\epsilon'_{\text{NP}}$  scenario, we find that one can accommodate simultaneously the  $h_\varepsilon$ ,  $h_{\varepsilon'}$  and  $h_{d_n}$  constraints only for  $s_s s_d = 1$ ; this is needed to avoid a  $\pi$  shift which would lead to a cancelation between the two terms in Eq. (56). By inspection one finds also the condition  $\text{sgn } \alpha = s_d s_t$ , so that for numerical convenience, one can restrict the analysis to the “log”-variable  $a = \tanh^{-1}[(2s_d s_t \alpha / \pi) - 1] \in (-\infty, \infty)$ . Finally, one finds that solutions exist only in four cases:  $\{1, 1, 1, 1, 1\}$ ,  $\{1, 1, 1, -1, -1\}$ ,  $\{-1, -1, -1, 1, 1\}$ ,  $\{-1, -1, -1, -1, -1\}$ , the last two being just replicas of the first two. The simultaneous experimental constraints produce allowed regions in the  $M_{W_R} - t_\beta - a$  space, which are depicted in Fig. 6. The numerical analysis is carried out for central values of the matrix elements as well as for the enlarged conservative range, left and right frames of Fig. 6 respectively. In the latter case solutions are found for four sign combinations more. When the allowed volumes are projected on the  $M_{W_R} - t_\beta$  plane, Fig. 5 is finally obtained.

A similar procedure is followed for the  $\epsilon'_{\text{SM}}$  scenario, where all 32 sign choices and both  $\text{sgn } \alpha = \pm 1$  contribute. Here the lowest bound on the LR scale is found in the subset with  $s_s s_d = 1$ , where the  $h_\varepsilon$  constraint can be satisfied.

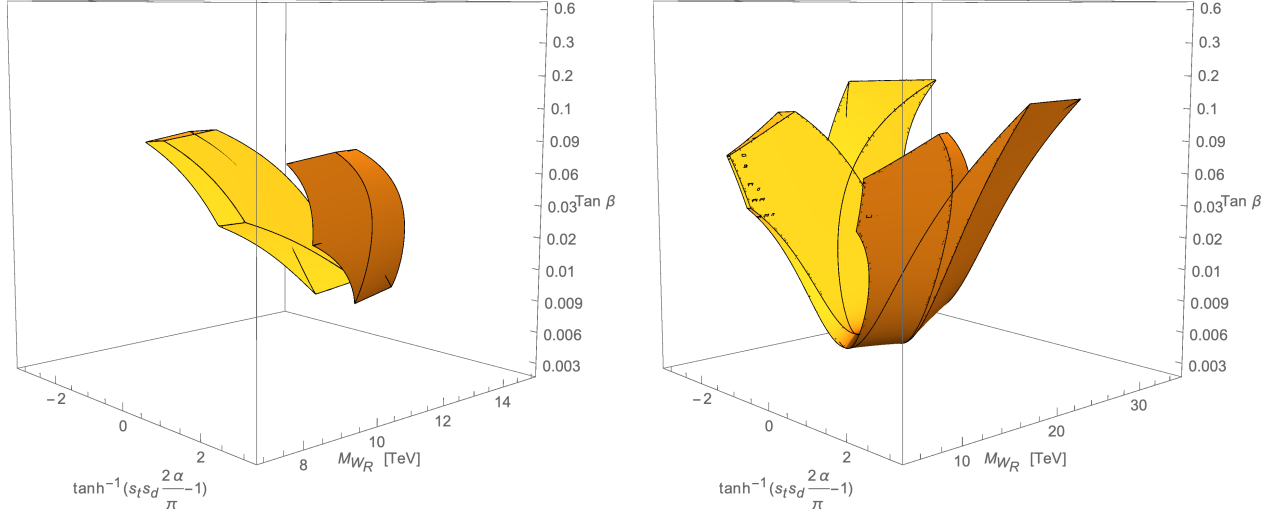


FIG. 6. Case of  $\mathcal{P}$ : The allowed region in the  $M_{W_R} - t_\beta - \alpha$  space for the  $\epsilon'_{NP}$  scenario.

---

[1] S. L. Glashow, J. Iliopoulos, and L. Maiani, “Weak Interactions with Lepton-Hadron Symmetry”, *Phys. Rev.* **D2** (1970) 1285–1292.

[2] M. Kobayashi and T. Maskawa, “CP Violation in the Renormalizable Theory of Weak Interaction”, *Prog. Theor. Phys.* **49** (1973) 652–657.

[3] J. Engel, M. J. Ramsey-Musolf, and U. van Kolck, “Electric Dipole Moments of Nucleons, Nuclei, and Atoms: The Standard Model and Beyond”, *Prog. Part. Nucl. Phys.* **71** (2013) 21–74, arXiv:1303.2371 [nucl-th].

[4] C. A. Baker *et al.*, “An Improved experimental limit on the electric dipole moment of the neutron”, *Phys. Rev. Lett.* **97** (2006) 131801, arXiv:hep-ex/0602020 [hep-ex].

[5] J. R. Ellis and M. K. Gaillard, “Strong and Weak CP Violation”, *Nucl. Phys.* **B150** (1979) 141–162.

[6] J. C. Pati and A. Salam, “Lepton Number as the Fourth Color”, *Phys. Rev.* **D10** (1974) 275–289. [Erratum: *Phys. Rev.* D11, 703 (1975)].

[7] R. N. Mohapatra and J. C. Pati, “Left-Right Gauge Symmetry and an Isoconjugate Model of CP Violation”, *Phys. Rev.* **D11** (1975) 566–571.

[8] R. N. Mohapatra and J. C. Pati, “A Natural Left-Right Symmetry”, *Phys. Rev.* **D11** (1975) 2558.

[9] G. Senjanović and R. N. Mohapatra, “Exact Left-Right Symmetry and Spontaneous Violation of Parity”, *Phys. Rev.* **D12** (1975) 1502.

[10] P. Minkowski, “ $\mu \rightarrow e\gamma$  at a Rate of One Out of  $10^9$  Muon Decays?”, *Phys. Lett.* **67B** (1977) 421–428.

[11] R. N. Mohapatra and G. Senjanović, “Neutrino Mass and Spontaneous Parity Nonconservation”, *Phys. Rev. Lett.* **44** (1980) 912. [231(1979)].

[12] G. Senjanović, “Spontaneous Breakdown of Parity in a Class of Gauge Theories”, *Nucl. Phys.* **B153** (1979) 334–364.

[13] R. N. Mohapatra and G. Senjanović, “Neutrino Masses and Mixings in Gauge Models with Spontaneous Parity Violation”, *Phys. Rev.* **D23** (1981) 165.

[14] V. Tello, M. Nemevšek, F. Nesti, G. Senjanović, and F. Vissani, “Left-Right Symmetry: from LHC to Neutrinoless Double Beta Decay”, *Phys. Rev. Lett.* **106** (2011) 151801, arXiv:1011.3522 [hep-ph].

[15] W.-Y. Keung and G. Senjanović, “Majorana Neutrinos and the Production of the Right-handed Charged Gauge Boson”, *Phys. Rev. Lett.* **50** (1983) 1427.

[16] M. Nemevšek, G. Senjanović, and V. Tello, “Connecting Dirac and Majorana Neutrino Mass Matrices in the Minimal Left-Right Symmetric Model”, *Phys. Rev. Lett.* **110** no. 15, (2013) 151802, arXiv:1211.2837 [hep-ph].

[17] G. Senjanović and V. Tello, “Probing Seesaw with Parity Restoration”, *Phys. Rev. Lett.* **119** no. 20, (2017) 201803, arXiv:1612.05503 [hep-ph].

[18] G. Senjanović and V. Tello, “Disentangling Seesaw in the Minimal Left-Right Symmetric Model”, arXiv:1812.03790 [hep-ph].

[19] J. C. Helo, H. Li, N. A. Neill, M. Ramsey-Musolf, and J. C. Vasquez, “Probing neutrino Dirac mass in left-right symmetric models at the LHC and next generation colliders”, *Phys. Rev.* **D99** no. 5, (2019) 055042, arXiv:1812.01630 [hep-ph].

[20] G. Beall, M. Bander, and A. Soni, “Constraint on the Mass Scale of a Left-Right Symmetric Electroweak Theory from the K(L) K(S) Mass Difference”, *Phys. Rev. Lett.* **48** (1982) 848.

[21] G. Ecker and W. Grimus, “CP Violation and Left-Right Symmetry”, *Nucl. Phys.* **B258** (1985) 328–360.

[22] A. Maiezza, M. Nemevšek, F. Nesti, and

G. Senjanović, “Left-Right Symmetry at LHC”, *Phys. Rev.* **D82** (2010) 055022, arXiv:1005.5160 [hep-ph].

[23] S. Bertolini, J. O. Eeg, A. Maiezza, and F. Nesti, “New physics in  $\epsilon'$  from gluomagnetic contributions and limits on Left-Right symmetry”, *Phys. Rev.* **D86** (2012) 095013, arXiv:1206.0668 [hep-ph]. [Erratum: *Phys. Rev.* D93,no.7,079903(2016)].

[24] S. Bertolini, A. Maiezza, and F. Nesti, “ $K \rightarrow \pi\pi$  hadronic matrix elements of left-right current-current operators”, *Phys. Rev.* **D88** no. 3, (2013) 034014, arXiv:1305.5739 [hep-ph].

[25] S. Bertolini, A. Maiezza, and F. Nesti, “Present and Future K and B Meson Mixing Constraints on TeV Scale Left-Right Symmetry”, *Phys. Rev.* **D89** no. 9, (2014) 095028, arXiv:1403.7112 [hep-ph].

[26] R. N. Mohapatra and G. Senjanović, “Natural Suppression of Strong p and t Noninvariance”, *Phys. Lett.* **79B** (1978) 283–286.

[27] R. D. Peccei and H. R. Quinn, “CP Conservation in the Presence of Instantons”, *Phys. Rev. Lett.* **38** (1977) 1440–1443. [,328(1977)].

[28] S. Weinberg, “A New Light Boson?”, *Phys. Rev. Lett.* **40** (1978) 223–226.

[29] F. Wilczek, “Problem of Strong  $P$  and  $T$  Invariance in the Presence of Instantons”, *Phys. Rev. Lett.* **40** (1978) 279–282.

[30] A. Maiezza and M. Nemevšek, “Strong P invariance, neutron electric dipole moment, and minimal left-right parity at LHC”, *Phys. Rev.* **D90** no. 9, (2014) 095002, arXiv:1407.3678 [hep-ph].

[31] A. Maiezza, M. Nemevšek, and F. Nesti, “Perturbativity and mass scales in the minimal left-right symmetric model”, *Phys. Rev.* **D94** no. 3, (2016) 035008, arXiv:1603.00360 [hep-ph].

[32] A. Maiezza, G. Senjanović, and J. C. Vasquez, “Higgs sector of the minimal left-right symmetric theory”, *Phys. Rev.* **D95** no. 9, (2017) 095004, arXiv:1612.09146 [hep-ph].

[33] M. Nemevšek, F. Nesti, and G. Popara, “Keung-Senjanović process at the LHC: From lepton number violation to displaced vertices to invisible decays”, *Phys. Rev.* **D97** no. 11, (2018) 115018, arXiv:1801.05813 [hep-ph].

[34] H. Gisbert and A. Pich, “Direct CP violation in  $K^0 \rightarrow \pi\pi$ : Standard Model Status”, *Rept. Prog. Phys.* **81** no. 7, (2018) 076201, arXiv:1712.06147 [hep-ph].

[35] A. J. Buras, “ $\epsilon'/\epsilon$ -2018: A Christmas Story”, arXiv:1812.06102 [hep-ph].

[36] V. Cirigliano, W. Dekens, J. de Vries, and E. Mereghetti, “An  $\epsilon'$  improvement from right-handed currents”, *Phys. Lett.* **B767** (2017) 1–9, arXiv:1612.03914 [hep-ph].

[37] W. Dekens, “ $\epsilon'$  from right-handed currents”, in *Proceedings, 52nd Rencontres de Moriond on Electroweak Interactions and Unified Theories: La Thuile, Italy, March 18-25, 2017*, pp. 187–194. 2017. arXiv:1708.00797 [hep-ph].

[38] N. Haba, H. Umeeda, and T. Yamada, “ $\epsilon'/\epsilon$  Anomaly and Neutron EDM in  $SU(2)_L \times SU(2)_R \times U(1)_{B-L}$  model with Charge Symmetry”, *JHEP* **05** (2018) 052, arXiv:1802.09903 [hep-ph].

[39] N. Haba, H. Umeeda, and T. Yamada, “Semialigned two Higgs doublet model”, *Phys. Rev.* **D97** no. 3, (2018) 035004, arXiv:1711.06499 [hep-ph].

[40] G. Senjanović and V. Tello, “Right Handed Quark Mixing in Left-Right Symmetric Theory”, *Phys. Rev. Lett.* **114** no. 7, (2015) 071801, arXiv:1408.3835 [hep-ph].

[41] G. Senjanović and V. Tello, “Restoration of Parity and the Right-Handed Analog of the CKM Matrix”, *Phys. Rev.* **D94** no. 9, (2016) 095023, arXiv:1502.05704 [hep-ph].

[42] G. Senjanović and P. Senjanović, “Suppression of Higgs Strangeness Changing Neutral Currents in a Class of Gauge Theories”, *Phys. Rev.* **D21** (1980) 3253.

[43] J. Basecq, L.-F. Li, and P. B. Pal, “Gauge Invariant Calculation of the  $K_L K_S$  Mass Difference in the Left-right Model”, *Phys. Rev.* **D32** (1985) 175.

[44] Flavour Lattice Averaging Group, S. Aoki *et al.*, “FLAG Review 2019”, arXiv:1902.08191 [hep-lat].

[45] A. J. Buras and J. Girstbacher, “Towards the Identification of New Physics through Quark Flavour Violating Processes”, *Rept. Prog. Phys.* **77** (2014) 086201, arXiv:1306.3775 [hep-ph].

[46] M. K. Gaillard and B. W. Lee, “Rare Decay Modes of the K-Mesons in Gauge Theories”, *Phys. Rev.* **D10** (1974) 897.

[47] A. Manohar and H. Georgi, “Chiral Quarks and the Nonrelativistic Quark Model”, *Nucl. Phys.* **B234** (1984) 189–212.

[48] A. G. Cohen and A. V. Manohar, “The  $\Delta I = 1/2$  Rule in the Chiral Quark Model”, *Phys. Lett.* **143B** (1984) 481–484.

[49] S. Bertolini, M. Fabbrichesi, and J. O. Eeg, “Theory of the CP violating parameter epsilon-prime / epsilon”, *Rev. Mod. Phys.* **72** (2000) 65–93, arXiv:hep-ph/9802405 [hep-ph].

[50] S. Bertolini, J. O. Eeg, M. Fabbrichesi, and E. I. Lashin, “The Delta I = 1/2 rule and B(K) at O( $p^{**4}$ ) in the chiral expansion”, *Nucl. Phys.* **B514** (1998) 63–92, arXiv:hep-ph/9705244 [hep-ph].

[51] V. Antonelli, S. Bertolini, J. O. Eeg, M. Fabbrichesi, and E. I. Lashin, “The Delta S = 1 weak chiral lagrangian as the effective theory of the chiral quark model”, *Nucl. Phys.* **B469** (1996) 143–180, arXiv:hep-ph/9511255 [hep-ph].

[52] S. Bertolini, M. Fabbrichesi, and E. Gabrielli, “The Relevance of the dipole Penguin operators in epsilon-prime / epsilon”, *Phys. Lett.* **B327** (1994) 136–144, arXiv:hep-ph/9312266 [hep-ph].

[53] S. Bertolini, J. O. Eeg, and M. Fabbrichesi, “Studying epsilon-prime / epsilon in the chiral quark model: gamma(5) scheme independence and NLO hadronic matrix elements”, *Nucl. Phys.* **B449** (1995) 197–228, arXiv:hep-ph/9409437 [hep-ph].

[54] ETM, M. Constantinou, M. Costa, R. Frezzotti, V. Lubicz, G. Martinelli, D. Meloni, H. Panagopoulos, and S. Simula, “ $K \rightarrow \pi$  matrix elements of the chromomagnetic operator on the lattice”, *Phys. Rev.* **D97** no. 7, (2018) 074501, arXiv:1712.09824 [hep-lat].

[55] A. J. Buras and J.-M. Gérard, “ $K \rightarrow \pi\pi$  and  $K - \pi$  Matrix Elements of the Chromomagnetic Operators from Dual QCD”, *JHEP* **07** (2018) 126, arXiv:1803.08052 [hep-ph].

[56] S. Bertolini, J. O. Eeg, and M. Fabbrichesi, “A New estimate of epsilon-prime / epsilon”, *Nucl. Phys.* **B476** (1996) 225–254, arXiv:hep-ph/9512356 [hep-ph].

[57] S. Bertolini, J. O. Eeg, M. Fabbrichesi, and E. I.

Lashin, “Epsilon-prime / epsilon at  $O(p^{**4})$  in the chiral expansion”, *Nucl. Phys.* **B514** (1998) 93–112, [arXiv:hep-ph/9706260 \[hep-ph\]](#).

[58] KTeV, A. Alavi-Harati *et al.*, “Observation of direct CP violation in  $K_{S,L} \rightarrow \pi\pi$  decays”, *Phys. Rev. Lett.* **83** (1999) 22–27, [arXiv:hep-ex/9905060 \[hep-ex\]](#).

[59] NA48, V. Fanti *et al.*, “A New measurement of direct CP violation in two pion decays of the neutral kaon”, *Phys. Lett.* **B465** (1999) 335–348, [arXiv:hep-ex/9909022 \[hep-ex\]](#).

[60] E. Pallante and A. Pich, “Strong enhancement of epsilon-prime / epsilon through final state interactions”, *Phys. Rev. Lett.* **84** (2000) 2568–2571, [arXiv:hep-ph/9911233 \[hep-ph\]](#).

[61] E. Pallante and A. Pich, “Final state interactions in kaon decays”, *Nucl. Phys.* **B592** (2001) 294–320, [arXiv:hep-ph/0007208 \[hep-ph\]](#).

[62] E. Pallante, A. Pich, and I. Scimemi, “The Role of final state interactions in epsilon-prime / epsilon”, *Int. J. Mod. Phys.* **A16S1B** (2001) 672–674, [arXiv:hep-ph/0010229 \[hep-ph\]](#).

[63] M. Buchler, G. Colangelo, J. Kambor, and F. Orellana, “Dispersion relations and soft pion theorems for  $K \rightarrow \pi\pi$ ”, *Phys. Lett.* **B521** (2001) 22–28, [arXiv:hep-ph/0102287 \[hep-ph\]](#).

[64] M. Buchler, G. Colangelo, J. Kambor, and F. Orellana, “A Note on the dispersive treatment of  $K \rightarrow \pi\pi$  with the kaon off-shell”, *Phys. Lett.* **B521** (2001) 29–32, [arXiv:hep-ph/0102289 \[hep-ph\]](#).

[65] G. Feinberg, P. Kabir, and S. Weinberg, “Transformation of muons into electrons”, *Phys. Rev. Lett.* **3** (1959) 527–530.

[66] A. J. Buras and J.-M. Gérard, “Final state interactions in  $K \rightarrow \pi\pi$  decays:  $\Delta I = 1/2$  rule vs.  $\epsilon'/\epsilon$ ”, *Eur. Phys. J.* **C77** no. 1, (2017) 10, [arXiv:1603.05686 \[hep-ph\]](#).

[67] J. Aebischer, A. J. Buras, and J.-M. Gérard, “BSM Hadronic Matrix Elements for  $\epsilon'/\epsilon$  and  $K \rightarrow \pi\pi$  Decays in the Dual QCD Approach”, [arXiv:1807.01709 \[hep-ph\]](#).

[68] W. A. Bardeen, A. J. Buras, and J. M. Gérard, “The Delta  $I = 1/2$  Rule in the Large N Limit”, *Phys. Lett.* **B180** (1986) 133–140.

[69] W. A. Bardeen, A. J. Buras, and J. M. Gérard, “The  $K \rightarrow \pi\pi$  Decays in the Large n Limit: Quark Evolution”, *Nucl. Phys.* **B293** (1987) 787–811.

[70] W. A. Bardeen, A. J. Buras, and J. M. Gérard, “A Consistent Analysis of the Delta  $I = 1/2$  Rule for K Decays”, *Phys. Lett.* **B192** (1987) 138–144.

[71] J. P. Fatelo and J. M. Gérard, “Current current operator evolution in the chiral limit”, *Phys. Lett.* **B347** (1995) 136–142.

[72] W. A. Bardeen, A. J. Buras, and J. M. Gérard, “The B Parameter Beyond the Leading Order of  $1/n$  Expansion”, *Phys. Lett.* **B211** (1988) 343–349.

[73] A. J. Buras, J.-M. Gérard, and W. A. Bardeen, “Large N Approach to Kaon Decays and Mixing 28 Years Later:  $\Delta I = 1/2$  Rule,  $\bar{B}_K$  and  $\Delta M_K$ ”, *Eur. Phys. J.* **C74** (2014) 2871, [arXiv:1401.1385 \[hep-ph\]](#).

[74] RBC/UKQCD, N. Garron, R. J. Hudspith, and A. T. Lytle, “Neutral Kaon Mixing Beyond the Standard Model with  $n_f = 2 + 1$  Chiral Fermions Part 1: Bare Matrix Elements and Physical Results”, *JHEP* **11** (2016) 001, [arXiv:1609.03334 \[hep-lat\]](#).

[75] RBC, UKQCD, P. A. Boyle, N. Garron, R. J. Hudspith, C. Lehner, and A. T. Lytle, “Neutral kaon mixing beyond the Standard Model with  $n_f = 2 + 1$  chiral fermions. Part 2: non perturbative renormalisation of the  $\Delta F = 2$  four-quark operators”, *JHEP* **10** (2017) 054, [arXiv:1708.03552 \[hep-lat\]](#).

[76] A. J. Buras and J.-M. Gérard, “Dual QCD Insight into BSM Hadronic Matrix Elements for  $K^0 - \bar{K}^0$  Mixing from Lattice QCD”, [arXiv:1804.02401 \[hep-ph\]](#).

[77] T. Blum *et al.*, “ $K \rightarrow \pi\pi$   $\Delta I = 3/2$  decay amplitude in the continuum limit”, *Phys. Rev.* **D91** no. 7, (2015) 074502, [arXiv:1502.00263 \[hep-lat\]](#).

[78] RBC, UKQCD, Z. Bai *et al.*, “Standard Model Prediction for Direct CP Violation in  $K \rightarrow \pi\pi$  Decay”, *Phys. Rev. Lett.* **115** no. 21, (2015) 212001, [arXiv:1505.07863 \[hep-lat\]](#).

[79] J. Aebischer, C. Bobeth, and A. J. Buras, “On the Importance of NNLO QCD and Isospin-breaking Corrections in  $\epsilon'/\epsilon$ ”, [arXiv:1909.05610 \[hep-ph\]](#).

[80] V. Cirigliano, H. Gisbert, A. Pich, and A. Rodriguez-Sanchez, “Isospin-Violating Contributions to  $\epsilon'/\epsilon$ ”, [arXiv:1911.01359 \[hep-ph\]](#).

[81] S. M. Barr, D. Chang, and G. Senjanović, “Strong CP problem and parity”, *Phys. Rev. Lett.* **67** (1991) 2765–2768.

[82] H. An, X. Ji, and F. Xu, “P-odd and CP-odd Four-Quark Contributions to Neutron EDM”, *JHEP* **02** (2010) 043, [arXiv:0908.2420 \[hep-ph\]](#).

[83] V. M. Khatsimovsky, I. B. Khriplovich, and A. S. Yelkhovsky, “Neutron Electric Dipole Moment, T Odd Nuclear Forces and Nature of CP Violation”, *Annals Phys.* **186** (1988) 1–14.

[84] F. Xu, H. An, and X. Ji, “Neutron Electric Dipole Moment Constraint on Scale of Minimal Left-Right Symmetric Model”, *JHEP* **03** (2010) 088, [arXiv:0910.2265 \[hep-ph\]](#).

[85] J. Hisano, K. Tsumura, and M. J. S. Yang, “QCD Corrections to Neutron Electric Dipole Moment from Dimension-six Four-Quark Operators”, *Phys. Lett.* **B713** (2012) 473–480, [arXiv:1205.2212 \[hep-ph\]](#).

[86] E. Braaten, C.-S. Li, and T.-C. Yuan, “The Evolution of Weinberg’s Gluonic CP Violation Operator”, *Phys. Rev. Lett.* **64** (1990) 1709.

[87] D. Chang, T. W. Kephart, W.-Y. Keung, and T. C. Yuan, “The Chromoelectric dipole moment of the heavy quark and purely gluonic CP violating operators”, *Phys. Rev. Lett.* **68** (1992) 439–442.

[88] D. Chang, T. W. Kephart, W.-Y. Keung, and T. C. Yuan, “An Effective field theory for the neutron electric dipole moment”, *Nucl. Phys.* **B384** (1992) 147–167.

[89] J. Brod and E. Stamou, “Electric dipole moment constraints on CP-violating heavy-quark Yukawas at next-to-leading order”, [arXiv:1810.12303 \[hep-ph\]](#).

[90] J. Hisano, J. Y. Lee, N. Nagata, and Y. Shimizu, “Reevaluation of Neutron Electric Dipole Moment with QCD Sum Rules”, *Phys. Rev.* **D85** (2012) 114044, [arXiv:1204.2653 \[hep-ph\]](#).

[91] T. Chupp, P. Fierlinger, M. Ramsey-Musolf, and J. Singh, “Electric dipole moments of atoms, molecules, nuclei, and particles”, *Rev. Mod. Phys.* **91** no. 1, (2019) 015001, [arXiv:1710.02504 \[physics.atom-ph\]](#).

[92] M. A. Shifman, A. I. Vainshtein, and V. I. Zakharov, “Can Confinement Ensure Natural CP Invariance of

Strong Interactions?”, *Nucl. Phys.* **B166** (1980) 493–506.

[93] D. A. Demir, M. Pospelov, and A. Ritz, “Hadronic EDMs, the Weinberg operator, and light gluinos”, *Phys. Rev.* **D67** (2003) 015007, [arXiv:hep-ph/0208257 \[hep-ph\]](https://arxiv.org/abs/hep-ph/0208257).

[94] X.-G. He and B. McKellar, “Large contribution to the neutron electric dipole moment from a dimension-six four quark operator”, *Phys. Rev.* **D47** (1993) 4055–4058.

[95] A. Pich and E. de Rafael, “Strong CP violation in an effective chiral Lagrangian approach”, *Nucl. Phys.* **B367** (1991) 313–333.

[96] K. Ottnad, B. Kubis, U. G. Meissner, and F. K. Guo, “New insights into the neutron electric dipole moment”, *Phys. Lett.* **B687** (2010) 42–47, [arXiv:0911.3981 \[hep-ph\]](https://arxiv.org/abs/0911.3981).

[97] F.-K. Guo and U.-G. Meissner, “Baryon electric dipole moments from strong CP violation”, *JHEP* **12** (2012) 097, [arXiv:1210.5887 \[hep-ph\]](https://arxiv.org/abs/1210.5887).

[98] C.-Y. Seng, J. de Vries, E. Mereghetti, H. H. Patel, and M. Ramsey-Musolf, “Nucleon electric dipole moments and the isovector parity- and time-reversal-odd pion-nucleon coupling”, *Phys. Lett.* **B736** (2014) 147–153, [arXiv:1401.5366 \[nucl-th\]](https://arxiv.org/abs/1401.5366).

[99] E. E. Jenkins and A. V. Manohar, “Chiral corrections to the baryon axial currents”, *Phys. Lett.* **B259** (1991) 353–358.

[100] T. Fuchs, J. Gegelia, G. Japaridze, and S. Scherer, “Renormalization of relativistic baryon chiral perturbation theory and power counting”, *Phys. Rev.* **D68** (2003) 056005, [arXiv:hep-ph/0302117 \[hep-ph\]](https://arxiv.org/abs/hep-ph/0302117).

[101] A. Maiezza, M. Nemevšek, and F. Nesti, “Lepton Number Violation in Higgs Decay at LHC”, *Phys. Rev. Lett.* **115** (2015) 081802, [arXiv:1503.06834 \[hep-ph\]](https://arxiv.org/abs/1503.06834).

[102] R. Ruiz, “Lepton Number Violation at Colliders from Kinematically Inaccessible Gauge Bosons”, *Eur. Phys. J.* **C77** no. 6, (2017) 375, [arXiv:1703.04669 \[hep-ph\]](https://arxiv.org/abs/1703.04669).

[103] T. Inami and C. S. Lim, “Effects of Superheavy Quarks and Leptons in Low-Energy Weak Processes  $k(L)$  to  $\mu$  anti- $\mu$ ,  $K^+$  to  $\pi^+$  Neutrino anti-neutrino and  $K^0$  - anti- $K^0$ ”, *Prog. Theor. Phys.* **65** (1981) 297. [Erratum: *Prog. Theor. Phys.* 65, 1772 (1981)].

[104] P. L. Cho and M. Misiak, “ $b$  to  $s$  gamma decay in  $SU(2)$ -L x  $SU(2)$ -R x  $U(1)$  extensions of the Standard Model”, *Phys. Rev.* **D49** (1994) 5894–5903, [arXiv:hep-ph/9310332 \[hep-ph\]](https://arxiv.org/abs/hep-ph/9310332).

[105] A. J. Buras, “Weak Hamiltonian, CP violation and rare decays”, in *Probing the standard model of particle interactions. Proceedings, Summer School in Theoretical Physics, NATO Advanced Study Institute, 68th session, Les Houches, France, July 28-September 5, 1997. Pt. 1, 2*, pp. 281–539. 1998. [arXiv:hep-ph/9806471 \[hep-ph\]](https://arxiv.org/abs/hep-ph/9806471).

[106] M. Misiak and M. Munz, “Two loop mixing of dimension five flavor changing operators”, *Phys. Lett.* **B344** (1995) 308–318, [arXiv:hep-ph/9409454 \[hep-ph\]](https://arxiv.org/abs/hep-ph/9409454).

[107] G. Degrassi, E. Franco, S. Marchetti, and L. Silvestrini, “QCD corrections to the electric dipole moment of the neutron in the MSSM”, *JHEP* **11** (2005) 044, [arXiv:hep-ph/0510137 \[hep-ph\]](https://arxiv.org/abs/hep-ph/0510137).

[108] S. Scherer and M. R. Schindler, “A Primer for Chiral Perturbation Theory”, *Lect. Notes Phys.* **830** (2012) pp.1–338.